Relic Groundwater and Mega Drought Confound Interpretations of Water Sustainability and Lithium Extraction in Arid Lands

Brendan J. Moran[1], David F. Boutt[1], Sarah V. McKnight[1], Jordan Jenckes[2], Lee Ann Munk[2], Daniel Corkran[1], and Alexander Kirshen[1]

[1]University of Massachusetts Amherst
[2]University of Alaska Anchorage

November 23, 2022

Abstract

Demand for lithium for batteries is growing rapidly with the global push to decarbonize energy systems. The Salar de Atacama, Chile holds ~42% of the planet's reserves in the form of brines hosted in massive evaporite aquifers. The mining of these brines and associated freshwater use has raised concerns over the sustainability of lithium extraction, yet large uncertainties remain regarding fundamental aspects of governing hydrological processes in these environments. This incomplete understanding has led to the perpetuation of misconceptions about what constitutes sustainable or renewable water use and therefore what justifies responsible allocation. We present an integrated hydrological assessment using tritium and stable oxygen & hydrogen isotopes paired with remotely sensed and terrestrial hydroclimate data to define unique sources of water distinguished by their residence time, physical characteristics, and connectivity to modern climate. Our results describe the impacts of major drought on surface and groundwaters and demonstrate that nearly all inflow to the basin is composed of water recharged >65 years ago. Still, modern precipitation is critical to sustaining important wetlands around the salar. Recent large rain events have increased surface water and vegetation extents and terrestrial water storage while mining-related water withdrawals have continued. As we show in this basin, poor conceptualizations of these complex hydrological systems have perpetuated the misallocation of water and the misattribution of impacts. These fundamental issues apply to many similar regions globally. Our new framework for hydrological assessment in these arid basins moves beyond calculating gross inputs-outputs at a steady-state to include all compartmentalized stores that constitute "modern" budgets.

Earth's Future

Relic Groundwater and Mega Drought Confound Interpretations of Water Sustainability and Lithium Extraction in Arid Lands

Brendan J. Moran[1] 0000-0002-9862-6241, David F. Boutt[1] 0000-0003-1397-0279, Sarah V. McKnight[1] 0000-0002-6013-193X, Jordan Jenckes[2] 0000-0002-1811-3076, Lee Ann Munk[2] 0000-0003-2850-545X, Daniel Corkran[1] 0000-0001-6168-8281, Alexander Kirshen[1] 0000-0003-2015-4085

[1]Department of Geosciences, University of Massachusetts Amherst

[2]Department of Geological Sciences, University of Alaska Anchorage

Corresponding author: Brendan Moran, bmoran@geo.umass.edu

Keywords: Salar de Atacama, Chile; Tritium; Groundwater Sustainability; Hydroclimate; Water Budget; Lithium Brine

Key Points:

- Freshwater inflows and the modern water budget at Salar de Atacama are dominated by relic groundwater.
- A long-term mega drought coincident with increases in groundwater extraction complicates the attribution of specific anthropogenic environmental impacts.
- Freshwater use and allocated water rights at the Salar de Atacama appear to not meet sustainable metrics.

Abstract

Demand for lithium for batteries is growing rapidly with the global push to decarbonize energy systems. The Salar de Atacama, Chile holds ~42% of the planet's reserves in the form of brines hosted in massive evaporite aquifers. The mining of these brines and associated freshwater use has raised concerns over the sustainability of lithium extraction, yet large uncertainties remain regarding fundamental aspects of governing hydrological processes in these environments. This incomplete understanding has led to the perpetuation of misconceptions about what constitutes sustainable or renewable water use and therefore what justifies responsible allocation. We present an integrated hydrological assessment using tritium and stable oxygen & hydrogen isotopes paired with remotely sensed and terrestrial hydroclimate data to define unique sources of water distinguished by their residence time, physical characteristics, and connectivity to modern climate. Our results describe the impacts of major drought on surface and groundwaters and demonstrate that nearly all inflow to the basin is composed of water recharged >65 years ago. Still, modern precipitation is critical to sustaining important wetlands around the salar. Recent large rain events have increased surface water and vegetation extents and terrestrial water storage while mining-related water withdrawals have continued. As we show in this basin, poor conceptualizations of these complex hydrological systems have perpetuated the misallocation of water and the misattribution of impacts. These fundamental issues apply to many similar regions globally. Our new framework for hydrological assessment in these arid basins moves beyond calculating gross inputs-outputs at a steady-state to include all compartmentalized stores that constitute "modern" budgets.

Plain Language Summary

Lithium is a critical resource for the green energy transition as the primary component in lithium-ion batteries. Most of the planet's resources occur in dry, water-scarce environments, like Salar de Atacama in Chile, where ~42% of the world's supply exists. The lithium resides in very salty groundwater (brine) beneath its salt flat. Large amounts of brine along with some freshwater are extracted to recover lithium, and as the world requires more, there is increasing scrutiny of water use and resulting environmental impacts. Yet, persistent gaps remain regarding our fundamental understanding of how and where water moves in these environments and therefore the impacts that its extraction may have on surrounding ecosystems and communities.

We employ a combination of satellite and ground-based hydrological and climatological data paired with water isotopes to comprehensively assess changes in the distribution and movement of groundwater and surface waters. Our results show that a major drought and subsequent wetter period are the primary drivers of surface hydrology changes over this period. We also show that most of the water here is very old, highlighting the shortcomings of current water allocations in the region, which assume that most of the water in the system is relatively young. This work presents a data-driven framework that for the first time allows water sustainability and lithium extraction to be adequately assessed in these arid regions.

1. Introduction

Water allocation and consumption are at the center of the debate surrounding resource extraction in many watersheds globally (Boulay et al., 2018; Pfister et al., 2009; Ridoutt & Pfister, 2010; Wada et al., 2017; Zipper et al., 2020). In particular, the extraction of lithium brines and associated freshwater use in arid regions have recently drawn the attention of many stakeholders seeking to understand the environmental impacts of the transition to green energy along the lithium-ion battery supply chain (Gajardo & Redón, 2019; Gutiérrez et al., 2018; Sonter et al., 2020). Lithium mining has a remarkably spatially explicit water scarcity footprint (Schomberg et al., 2021) because exploited deposits have a strong connection to climate aridity (Munk et al., 2016). In northern Chile, which globally has the largest lithium reserve (Munk et al., 2016), fresh groundwater has reached unprecedented demand and market prices (Oyarzún & Oyarzún, 2011). Yet for the Salar de Atacama (SdA), which represents the largest single recoverable lithium resource in the world with approximately 42% of the global reserve base as of 2021 (Cabello, 2021, USGS, 2022), no studies to date have constrained the capability of the basin's water budget to meet current water demands, possibly because of notable uncertainty between permitted water use and actual extraction (Babidge et al., 2019), and the lack of legitimate sustainability metrics. Rapidly increasing global demand for lithium (Kesler et al., 2012; Ambrose and Kendall, 2020) coupled with the hydrologic imbalance between recharge and discharge in this basin (Boutt et al., 2021) therefore necessitates a critical examination of water sustainability in light of anthropogenic and climatic pressures on these environments.

Human activities including mineral resource extraction and other water consumption (irrigation, domestic use) have large impacts on the water budgets of basins (AghaKouchak et

al., 2021; Wang et al., 2018). In arid environments especially, attribution of hydrologic impacts from such activities can be difficult due to large interannual precipitation variability and the lack of long-term, continuous instrumental records (Ashraf et al., 2021; Bierkens & Wada, 2019; Rivera et al., 2021). Changes in rainfall patterns and timing lead to complex fluctuations in surface water features and water table positions (Fan et al., 2013). Yet the common practice of monitoring for mining purposes consists of baseline measurements that are only collected for a few years before the start of projects and therefore do not allow for the assessment of the natural variability of hydrologic systems. Furthermore, the over-reliance on steady-state water budget accounting for management, rather than focusing on the specific inventory of water resources has resulted in substantial misunderstandings of these systems (McDonnell, 2017).

The importance of highly variable precipitation events and the small margin for error in water-limited environments makes it challenging to responsibly allocate water resources in these basins (Stonestrom & Harrill, 2007; Schaffer et al., 2019; Somers & McKenzie, 2020). Pluvial events and droughts along with their timing have strong control on the inferred hydrologic conditions of a particular watershed and water allocation (Houston & Hart, 2004; Ferrero & Villalba, 2019). Reliance on outmoded methods of accounting by the water authorities in SdA, in particular, evokes questions of whether water allocations have ever met sustainable metrics (Bredehoeft, 2002). Having a data-driven and justifiable scientific understanding of the hydrological regime is key to avoiding mistakes in system conceptualization, water allocation, and the propagation of misinformation in the public domain.

In these arid environments surface water discharge is dominated by either infrequent precipitation events, seasonal snowmelt runoff, or spring discharge and stream baseflow fed by groundwater (Masbruch et al., 2016). These three sources of water can have very different residence times and respond distinctly to changes in hydrological conditions. In addition, long-term aridity develops deep water tables and long flow paths, creating effective catchment areas that are often much larger than topographic watersheds (Liu et al., 2020; Gleeson et al., 2011). The groundwater near basin floors, therefore, tends to be dominated by long transit times (Schaller & Fan, 2009). The resulting surface and groundwater bodies in these systems can display substantial variability in source water and responses to perturbations over relatively small spatial scales. Understanding how different water compartments respond to interannual hydrological variability is therefore critical to resource understanding and management.

The work presented here integrates remotely sensed and ground-based climate data, physical hydrological assessments, and tritium-based residence time analyses to determine changes in water storage and fluxes in the SdA catchment. We document that the region has experienced major paleo-hydrological changes in the past that left behind relic (premodern or fossil) waters, which naturally sustain modern wetland complexes but are being exploited for industrial use. We show that over the last two decades a region-wide Mega Drought has further impacted water availability concomitant with increased water use and resource extraction (Garreaud et al., 2020). In more recent years, a shift to wetter and more variable conditions has, in fact, increased total basin water storage and expanded many natural surface water features. Clear assessments and attribution of impacts are challenging because of the confounding nature of climate variability and human water use but are essential to evaluating the sustainability of lithium resource devolvement.

2. Background

2.1. Climate

The SdA basin lies within the Preandean Depression at the margin of the hyperarid Atacama Desert core to the west, and the Western Cordillera and Altiplano-Puna Plateau to the east. The region surrounding the basin has become known as the Lithium Triangle as it contains most of the world's lithium resources (**Figure 1a**). Annual precipitation west of the Andes including the floor of SdA averages only 2-15 mm/year, while many areas above 4,500 masl can average 250-300 mm/year (DGA, 2013; Houston, 2006). Of this high-elevation precipitation, approximately 50 to 80 mm of snow water equivalent falls each year; however, much of this liquid sublimates or evaporates before infiltrating due to high insolation and low relative humidity (Vuille & Ammann, 1997; Kinnard et al., 2020). Recent evidence indicates that this dry-season snowfall has decreased by ~10% per decade since the 1980s (Cordero et al., 2019). Most of the annual precipitation in the basin (>80%) occurs in summer, from December through March, and is inherently episodic, occurring in clusters of about a week when large amounts of rainfall can occur over short periods (Garreud et al., 2003; Valdivielso et al., 2020). The condensed and convective nature of rainfall means that annual totals can significantly vary year-to-year, especially at lower elevations (Garreaud et al., 2003). Widespread diffuse recharge likely

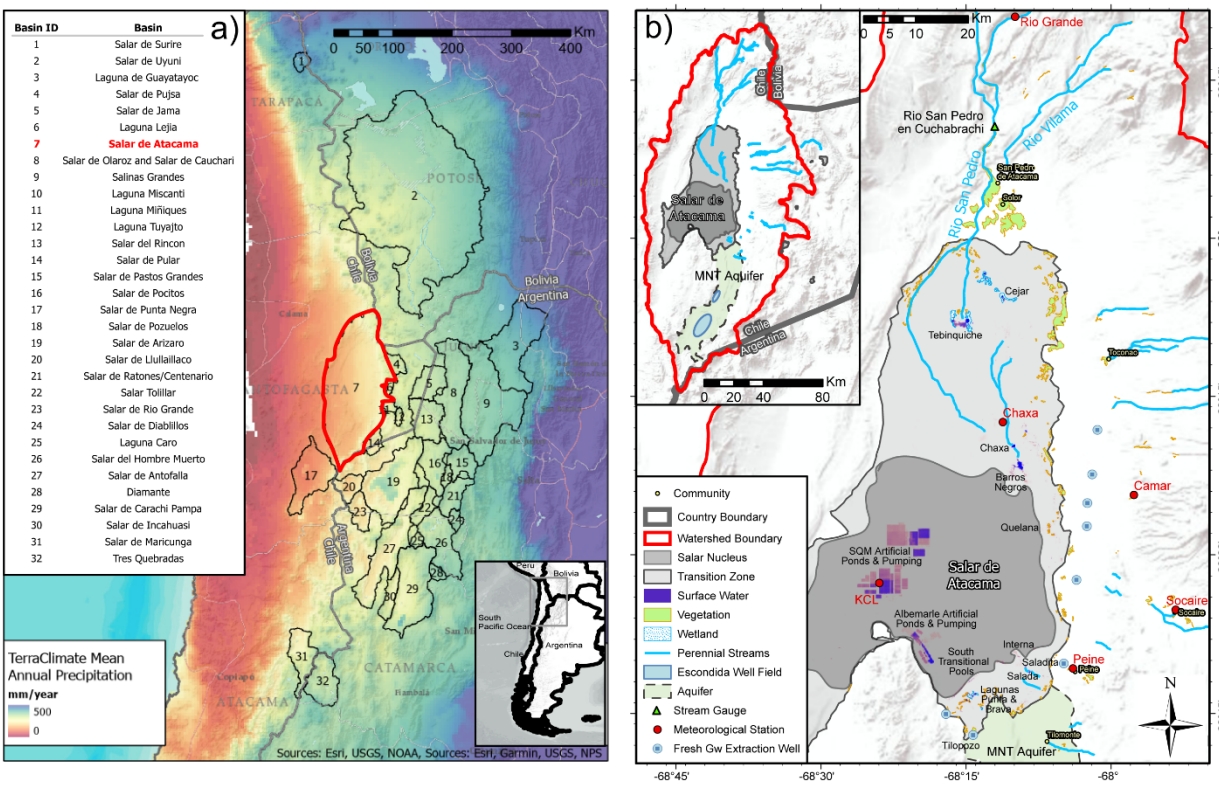

Figure 1. Major lithium-bearing basins of the Dry Andean Plateau of South America. **(a)** The regional mean annual precipitation of the region and the SdA basin topographic watershed are outlined in red. **(b)** Inset map of the SdA basin and its hydrological features. The salar nucleus, transition zone, surface waters, vegetated wetlands, and perennial streams are outlined. Meteorological stations and the stream gauge are labeled along with the location of fresh groundwater extraction wells. The MNT aquifer is highlighted in green, and streams (rivers) are in blue.

only occurs at elevations above ~3,900 masl where rainfall surpasses known thresholds required for recharge (e.g., Scanlon et al., 2006; Houston, 2007, 2009; Boutt et al., 2016). However, infrequent high-intensity rainfall events likely produce focused surface flows and groundwater recharge in parts of the basin (Houston, 2006; Boutt et al., 2016). No permanent ice exists at present within the recharge area of SdA except for some localized rock glaciers that may be present above 4,500 masl (Schaffer et al., 2019; Jones et al., 2019).

Paleoclimate records in the region indicate that hyperarid to arid climates dominated for at least the past 53 ka (Bobst et al. 2001; Godfrey et al. 2003), with at least four periods wetter than the modern occurring since 106 ka (Gayo et al. 2012). The most recent of these pluvial periods, around the last glacial maximum, increased precipitation by 2-3 times modern amounts and lasted for several thousand years (Placzek et al. 2013). Records from multiple Altiplano lakes indicate lake levels increased by tens of meters during this period (Blard et al., 2011), and

Laguna Lejía approximately 40 km east of the salar at 4,325 masl was ~25 m higher than today, which would require double the modern precipitation rate, up to 500 mm/year (Grosjean et al., 1995; Grosjean & Núñez, 1994). The climate around SdA has been drier since the mid-Holocene based on evidence that water tables were below the ground surface at paleo-wetland sites and observations from sediment cores from the salar nucleus (Rech et al. 2003; Quade et al. 2008; Placzek et al. 2013). These wet periods dramatically altered the hydrological and ecological conditions in the basin (Pfeiffer et al., 2018), and the effects are likely still evident in the modern hydrological system in the form of transient groundwater storage changes within the deep and extensive regional aquifers responding over 100-10,000-year time scales (Moran et. al., 2019).

2.2. Basin Hydrology

The SdA basin catchment is a large and deep topographic depression of about 17,000 km^2 that spans a vertical profile of >3500 meters, its basin floor (2,900 km^2) is covered mostly by evaporite sediments with some clastic material and hosts a vast halite nucleus covering about 1,700 km^2. The water budget and physical hydrology of the SdA region have been the focus of several recent studies (Houston, 2007, Corenthal et al., 2016, Munk et al., 2018, Boutt et al., 2021). A summary of the key hydrological attributes at SdA is introduced here (**Figure *1b***). Due to the extreme aridity, there is only one river (Rio San Pedro) that directly feeds the floor of the basin, while several smaller streams infiltrate completely before reaching the basin floor. About 2/3's of inflow to the basin is from low to mid-elevation (~2,450-2,600 masl) spring-fed streams and diffuse groundwater inflow through tabular ignimbrite sheets and alluvial fans. These inflows that discharge above the basin floor re-infiltrate into the permeable alluvial fan deposits before at least some portion emerges again as springs near the salar floor. Water leaves the basin through direct evaporation (and limited transpiration) in marginal areas herein called transition zones. The intense evaporation that far outpaces precipitation on the basin floor has created a massive evaporite deposit (Corenthal et al., 2016) and brine body. The high-density brine interacts with inflowing freshwater to create density-driven groundwater flow conditions and fresh groundwater upwelling, which in turn results in freshwater discharge from the low elevation springs (McKnight et al., 2021). The halite-rich brine aquifer, within the nucleus, is currently being exploited for its lithium resource (Munk et al., 2016). Geochemical evidence and physical hydrogeological conceptualization (Munk et al., 2021) do not support a source of

183 modern groundwater inflow to the brine aquifer, while Boutt et al. (2016) document recharge to
184 the brine body through direct precipitation and infiltration of surface waters that accumulate
185 along the halite nucleus margin.

186 In a recent contribution, Boutt et al. (2021) presented a comprehensive review of the
187 water budget and discussed different conceptualizations of basin hydrology. They show that the
188 amount of observed water inflow to the basin floor is a large percentage (~25%) of estimated
189 total modern precipitation inputs. Basin yields approaching even 4-8% of the total precipitation
190 are not realistic in arid environments with deep water tables, thick vadose zones, and large
191 evaporative demands (Scanlon et al., 2002). Following Corenthal et al. (2016) that showed the
192 annual modern hydrologic budget within the topographic watershed does not close and
193 implicated interbasin groundwater flow and relic or "fossil" water inflows to close the budget,
194 Moran et al. (2019) provided geochemical and hydrophysical evidence to support this
195 conclusion. Regardless of the mechanism invoked to balance the budget, these results
196 significantly impact how the basin water budget must be treated and managed.

197 **2.3. Water Use**

198 Water use in SdA has a long history that originates with indigenous communities, known
199 as the Atacameños, who have been using surface waters for agriculture and domestic uses for
200 millennia (Babidge et al., 2019). Only in the past three decades has water been managed by the
201 national governing agency known as Dirección General de Aguas (DGA) as groundwater
202 extraction for mining purposes increased (Anderson et al., 2002). During that period, allocated
203 water rights by the DGA resulted in the development of groundwater extraction wells. Before
204 this, water was primarily consumed from perennial streams and springs at the surface and almost
205 all non-industrial water use is still from these surface water sources. Water consumption
206 currently serves diverse purposes in the basin, including mining, agricultural, and domestic use
207 (DGA, 2013; Babidge, 2019). The understanding of actual consumption is limited to reported
208 pumping rates from industrial users and poorly constrained estimates of non-industrial use
209 (AMPHOS21, 2018). Thus, as we further show in this study, understanding water use is limited
210 to what is reported and permitted, and may not fully encompass total water use occurring in the
211 basin. Nevertheless, with currently available water use estimations, there exists no meaningful

212 analysis of whether this water use can be considered sustainable within the current water budget
213 framework.

214 ## 3. Methods and Approach

215 ### 3.1. Remote Sensing

216 This study utilizes multiple remotely sensed data sets to assess the recent hydrological
217 and climatological regimes at SdA. These include Landsat satellite imagery (spatial resolution of
218 30 meters with imagery every ~16 days), TerraClimate climatically-aided interpolation of
219 precipitation, and the Gravity Recovery & Climate Experiment (GRACE). To extract long-term
220 seasonal time series of surface water extent we utilized the Joint Research Centre (JRC) global
221 monthly water extent imagery (Pekel et al., 2016). Using GEE, we extracted a full series of
222 images from Landsat 5 & 7 Surface Reflectance Tier 1 (atmospherically corrected ETM sensor)
223 data for 1984 through 2020 and determined the number of pixels covered by vegetation from
224 which a total geographic area was calculated using a set of off-the-shelf functions provided by
225 the GEE API. This provides a time series of the total area covered by living or "green"
226 vegetation within the ROI. Further description of these methods and analysis of the reliability of
227 the TerraClimate dataset relative to other data products is included in the supplemental material
228 (**Text S1**).

229 To extend our hydroclimatic assessment we utilized data from GRACE which provides
230 Terrestrial Water Storage Anomaly (TWSA) at a monthly resolution based on small changes in
231 Earth's gravity field. The spatial resolution of the dataset is coarse (3.0° downscaled to 0.5°) but
232 is an excellent tool for assessing changes in total water storage at the basin scale (Reager et al.,
233 2013). Time series of TWSA (relative to a 2004-2009 baseline), presented as a liquid water
234 equivalent thickness, were produced for the SdA basin from monthly mass grids produced by
235 two centers: CSR (university of Texas/Center for Space Research) and JPL (NASA Jet
236 Propulsion Laboratory) publicly available from GRACE Tellus
237 (https://grace.jpl.nasa.gov/data/get-data/; Landerer, 2021).

3.2. Terrestrial Groundwater, Surface Water, and Precipitation Data

This study utilizes streamflow, precipitation, and groundwater level measurements from locations throughout the SdA catchment to assess changes in hydrologic conditions. We obtained streamflow records from the Rio San Pedro en Cuchabrachi stream gauge and precipitation records for the Camar, Peine, Rio Grande, and Socaire meteorological stations from the DGA (https://snia.mop.gob.cl/BNAConsultas/reportes) (**Figure *1b***). Additional precipitation records for the Chaxa and KCL meteorological stations came from the Sociedad Quimica y Minera S.A. (SQM) environmental monitoring database (https://www.sqmsenlinea.com/meteorology).

3.3. Water Residence Times

To assess spatially explicit water residence times within the hydrological system we utilize stable ($\delta^{18}O$ & $\delta^{2}H$) and radiogenic (^{3}H) isotopic tracers, along with dissolved chloride (Cl^-) in 106 water samples across the SdA catchment. These include surface and groundwaters collected during numerous field campaigns between October 2011 and March 2021. Samples were collected with a consistent, standardized procedure and in-situ measurements of temperature, specific conductance, and pH were made at each sampling location during collection. These data are presented in full in the supplemental material (**Table S1**) and a detailed analytical procedure is also provided (**Text S1**).

Physical Water Type Classification

Sampled waters were grouped into seven physical water types to facilitate the interpretation and communication of our results. These distinctions are based on extensive knowledge of the regional hydrogeology gathered during more than ten field campaigns, previously published works, and scrutiny of geochemical signatures (Munk et al., 2021). Nucleus Brines are groundwaters from the core of the halite-dominated brine aquifer, sampled at shallow depths <13 meters below ground level (mbgl), Marginal Brines are groundwaters from the margins of the brine aquifer, sampled at the water table (<2 mbgl). Transitional Pools are highly saline, shallow pools that form at the margin of the halite crust which grow and shrink rapidly primarily in response to precipitation events. These are often adjacent to (~1-2km away) but distinct from the Lagoons which include the culturally and ecologically important lagoons Brava,

Chaxa, and Tebinquiche. Many of these water bodies also grow and shrink seasonally and after precipitation events but are perennially extant. They are also quite shallow (<1m) but much less saline than the Transitional Pools. The basin inflow waters are separated into three groups; Streams are perennially flowing fresh surface waters, Inflow Groundwaters (Inflow Gw) are fresh to brackish waters sampled from wells upgradient of the salar transition zone, and Transition Zone Groundwaters are brackish to saline waters sampled at the water table within the salar transition zone.

Tritium Age Tracing Approach

The hydrological system at SdA is complex and heterogeneous on all scales, and large gaps exist in hydrogeological and hydroclimatological data coverage especially above the basin floor and on the adjacent plateau. Very deep water tables and rugged terrain make direct observation of the groundwater system impractical across much of the landscape, and long-term high-quality terrestrial monitoring of the hydroclimate is sparse. Therefore, highly parameterized models and tracers that require additional assumptions are not the most effective tools in this environment. Tracing the water molecule itself most accurately integrates small-scale variability with large-scale processes (Birkel et al., 2015; Buttle, 1994). Stable isotope ratios ($\delta^{18}O$, $\delta^{2}H$) and radioisotopes (^{3}H) in water offer many unique advantages in these systems (Cook & Bohlke, 2000; Kendall & Caldwell, 1998). Signatures of $\delta^{18}O$ & $\delta^{2}H$ in groundwater remain unchanged from the point of recharge until its re-emergence from the ground (Beria et al., 2018; Clark & Fritz, 1997; Kendall & McDonnell, 1998). Radioisotope signatures (^{3}H) are also conservative in this way but also follow a predictable decay (half-life of 12.32 years) during transit. To effectively utilize this tracer, we must constrain the ^{3}H content of modern precipitation as the modern recharge signature for inflows. This value, also presented by Boutt et al. (2016) and Moran et al. (2019), is determined to be 3.23 ± 0.6 TU (1σ) from five carefully chosen, amount weighted rain samples collected during 2013 and 2014. This value is within the range reported by others in the region (Cortecci et al., 2005; Grosjean et al., 1995; Herrera et al., 2016; Houston, 2002, 2007).

Widespread atmospheric nuclear bomb testing in the late 1950s and early ’60s created a large and unmistakable peak in global atmospheric ^{3}H concentrations which increased

concentrations in meteoric water globally by greater than an order of magnitude (Cartwright et al., 2017). This unmistakable signature allows for reliable differentiation between water recharged post-1955 and that emplaced before. We assume the modern value in meteoric water described above is representative of average precipitation from about 2000 to the present since the bomb peak signature is no longer resolvable after that date in the Southern Hemisphere (Rooyen et al., 2021). This background signature should also be representative of precipitation before the mid-1950s since the bomb peak had not yet occurred (Houston, 2007; Jasechko, 2016). Since the ^{3}H activity in any given sample is a bulk sample representing mixtures of unknown sources and respective amounts, we must be careful not to over-interpret specific ^{3}H activity values in individual samples. To ensure reliable and conservative interpretation we determine a "percent modern water" ratio in each sample as the ratio of background meteoric input activity to the activity measured in the sample. In this extreme, arid environment essentially all water reliably contains either very small amounts of measurable ^{3}H (<0.15 TU) or a substantial amount (>1.0 TU). Water recharged in 1955 before the bomb peak with a ^{3}H content of 3.23 ± 0.6 TU would have between 0.08 and 0.11 TU in July 2018, or 2-3% of the meteoric input value (Stewart et al., 2017). Due to the small but non-negligible analytical uncertainty (~0.02-0.07 TU at low activities) and potential very low levels of in-situ creation of ^{3}H, samples with these very small activities are herein considered to be effectively ^{3}H-dead waters or indistinguishable from zero. Waters registering such low activities are assumed to contain negligible volumes of water recharged post-bomb peak (1955), as even small amounts of water with higher activities would readily skew total activities in these ^{3}H-dead samples to an observable effect. Since most of the waters measured in this environment contain effectively no ^{3}H, our objective is not to directly estimate discrete mean residence time distributions but instead to describe the relative proportions of ^{3}H-dead to recent recharge (<65 years old) in these waters (Cartwright et al., 2017). This relative water age value allows for the reliable interpretation of connections to modern meteoric inputs, as well as the lack thereof.

3.4. Water Use Quantification

We compiled all available water use data within the SdA basin to develop a comprehensive basin-wide assessment of anthropogenic water use. The DGA maintains and publishes a national database of all water use permits in Chile. Several public reports analyzing

resource and reserve estimates of lithium have used this database to analyze possible impacts of water use (AMPHOS21, 2018). We utilize this DGA database along with communications with local communities to present and assess total freshwater allocation in SdA. To calculate estimated actual freshwater use in the basin, we used groundwater pumping rates from mining companies, available in public reports. A detailed description of how these data were collected is given in the supplemental material (**Text S1**)

4. Results

4.1. Climate, Hydrology, and Water Storage Changes

Precipitation

We characterize the climate regime at SdA since 1984 using the TerraClimate dataset and station-based meteorological data from the six longest and most complete records, identifying several distinct periods including two long-term droughts and three wet intervals (**Figure *2***). To properly frame these results, it's important to point out distinctions between the instrumental and remotely sensed records. First, TerraClimate represents an area-integrated mean annual accumulation value for the entire SdA topographic watershed, including the basin floor (~20% of the watershed area) which averages <15 mm/year. These data provide a reliable assessment of basin-scale climate and multi-annual trends but naturally smooth large interannual and spatial variations in precipitation. For instance, the SdA mean annual precipitation in the TerraClimate record (1958-2020) is 37 mm/year with a standard deviation of 18mm (**Figure *2***b). The longest and most complete record in the basin, Camar station (1979-2019) located about 400 meters above the basin floor recorded a mean of 43 mm/year with a standard deviation of 46 mm (**Figure *2***a). The interannual variability is larger than the mean annual precipitation at Camar, a feature common among station records in the basin. This basin spans about 150 km from north to south, thus precipitation at Rio Grande station near the northern end is consistently greater than at Socaire station in the southern part of the basin even though they are at the same elevation. The climate intervals presented here are intended to describe overall changes by correlating station data trends and basin-wide average amounts, but it's important to recognize that the timing and magnitude of these changes vary across the basin.

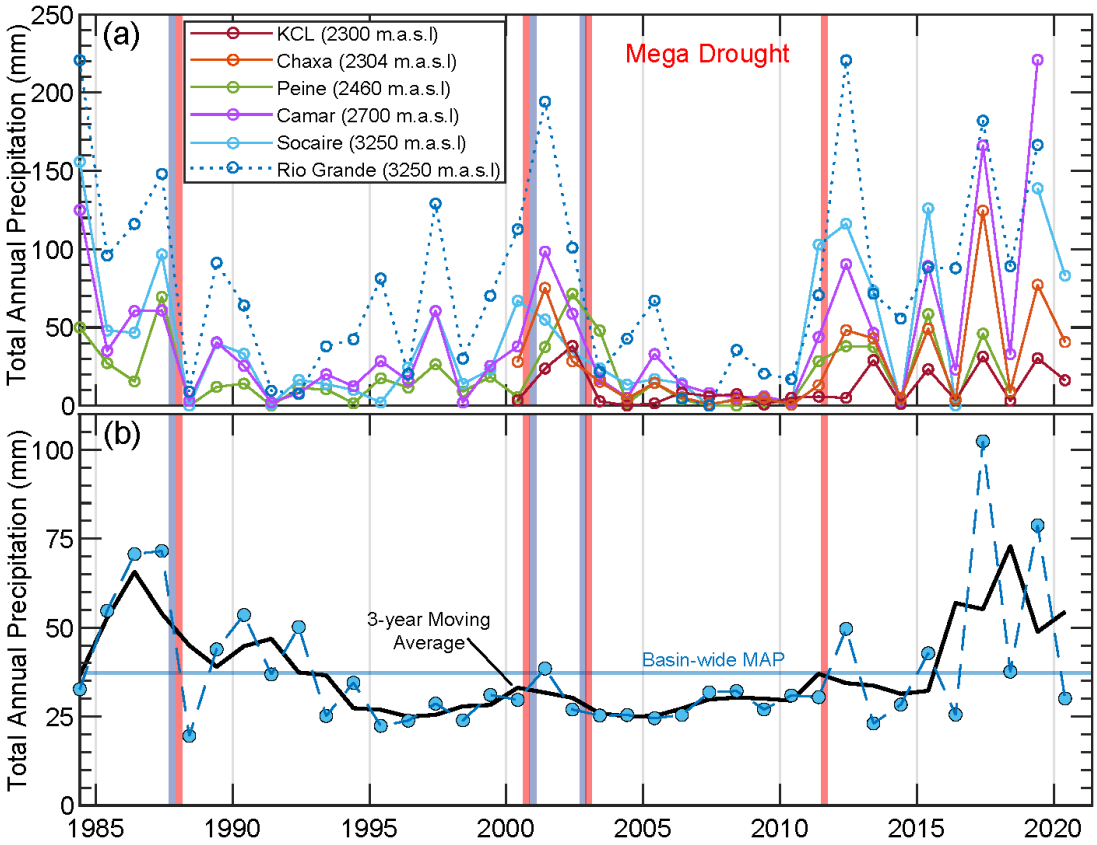

Figure 2. Annual precipitation from 1984-2020. Vertical red/blue bars represent major climate intervals identified. **(a)** Shows records from meteorological stations within the basin, the Rio Grande station record is a dotted line due to its location at the northern end of the basin. **(b)** The basin-wide area-integrated annual precipitation from the TerraClimate dataset with the 3-year moving average. The Mean Annual Precipitation (MAP) from the TerraClimate record (1958-present) is indicated by the blue horizontal line.

Localized and interannual variations are captured by station data; however, large events can be recorded at certain stations and barely register at others or occur several weeks apart. For instance, February-March of 2001 was one of the wettest periods on record in the north and northeast of the basin where Rio Grande (178mm), Chaxa (71 mm), and Camar (99mm) all recorded greater than double their mean annual precipitation in just a few weeks. The stations in the south and east recorded average or below-average precipitation that year, however, the following year Peine and KCL stations had their wettest year on record. When interpreting hydroclimate changes and their responses basin-wide we need to account for these spatial differences as well as the overall regime. Therefore, we define major long-term intervals and individual events that are registered basin-wide. These intervals provide a comprehensive and reliable picture of climatological changes in the basin over the last several decades which can be

then applied to describe and attribute corresponding natural responses within the hydrological system.

Five distinct climate intervals are identified since 1984, the most prominent of these is termed the 'Mega Drought' which began in 2003 following a period of less extreme drought and two very wet years. We identify this drought by consecutive years of annual precipitation deficits of between 12% and 33% in basin-wide precipitation over almost a decade, paired with strong decreases in precipitation across all stations after 2002. Due to the significance and region-wide nature of this phenomenon, it was labeled a Mega Drought by a recent study (Garreaud et al., 2020), and major deficits were also documented by researchers in northwestern Argentina during this period (Ferrero et al., 2019). Following the Mega Drought, the climate regime at SdA has become wetter but also significantly more variable, with several years of anomalously high precipitation followed by years of anomalously low totals. This recent period is punctuated by three of the largest widespread precipitation events in the instrumental record occurring in 2015, 2017, and 2019. From late January to early February 2019, every station in the basin recorded greater than their mean annual total over less than 3 weeks. This event particularly in the southern and eastern parts of the basin was the most significant precipitation event on record. These large events have become notably more common over the last decade and have major observable impacts on surface water bodies, wetland vegetation, and overall storage in the basin.

Hydrological Changes

Changes observed in the SdA hydrological system (i.e., surface waters, vegetation, and streamflow) and basin-scale TWSA correlate well with the climate intervals described above; however, there are important differences in timing and magnitude of response to rainfall and drought. Overall, during the drought periods average Surface Water Extent (SWE), vegetation extent, and TWSA are reduced and stable year-to-year, while during wet intervals and large precipitation events corresponding increases occur (**Figure *3***). SWE changes in the basin follow a seasonal cycle of larger winter extents, when potential evaporation is low, and reach yearly lows in the summer (**Figure *3***a). This annual behavior is out-of-phase with precipitation, predominantly between December and March, although it appears that after large events such as in 2001, 2017, and 2019, SWE responded strongly and quickly and did not recede fully until the

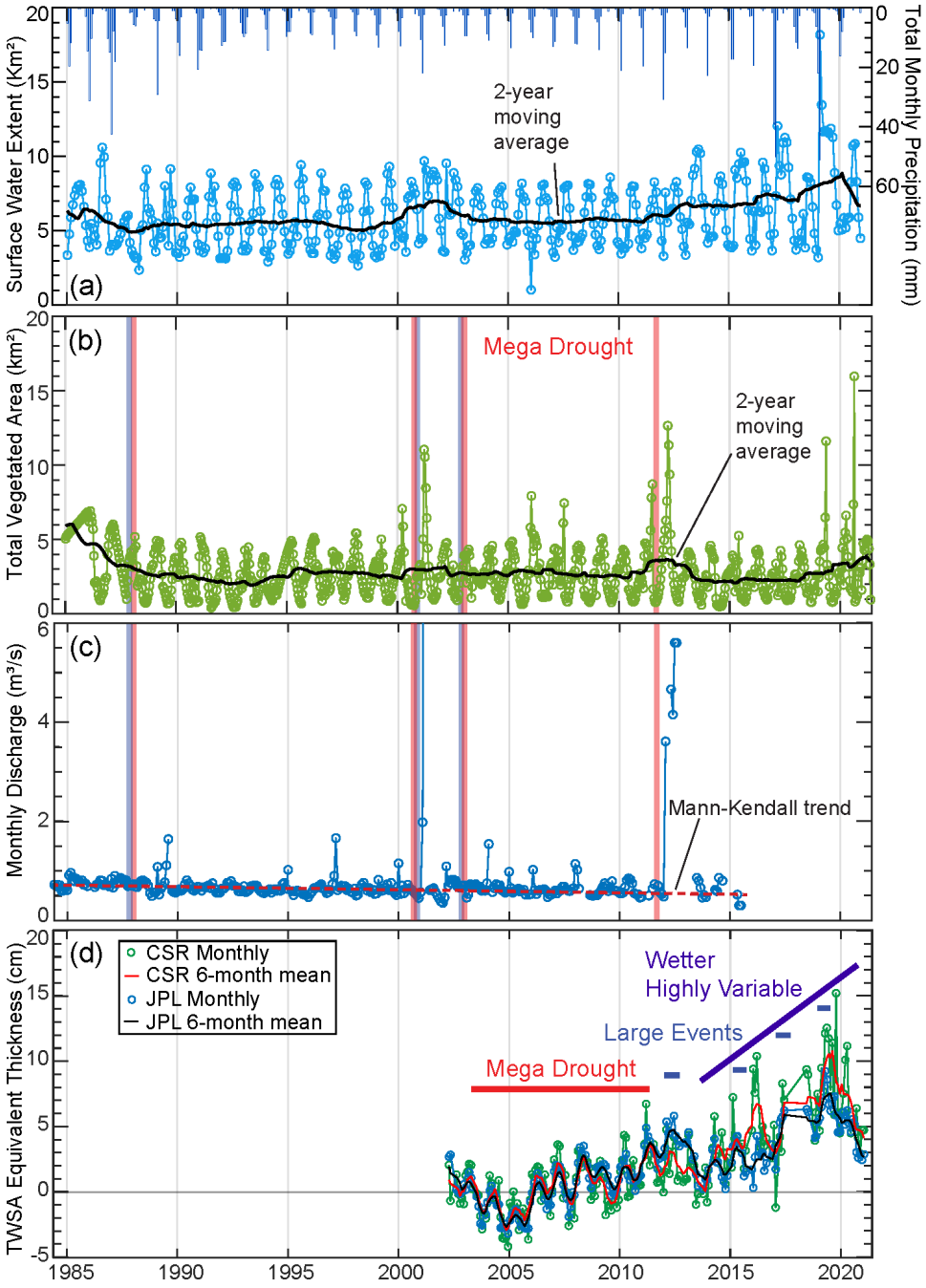

Figure 3. Changes in basin-wide hydrological conditions since 1985. **(a)** Total monthly surface water extent and TerraClimate total monthly precipitation, **(b)** total monthly extent of living vegetation, **(c)** average monthly discharge at the San Pedro stream gauge, and **(d)** GRACE-derived monthly terrestrial water storage anomaly equivalent thickness produced by JPL (green) and CSR (blue). Climate intervals are indicated with vertical bars and further detailed in **(d)** with the timing of large precipitation events.

following summer. Large increases in average SWE seen after 2012, which accelerated after 2015 are primarily the result of these events adding large pulses of water to the system. During

the Mega Drought period, average extents are consistently low, similar to the drought in the 1990s, however, the winter maximums are consistently lower than that period. Vegetation extents appear overall less variable than SWE, following an annual cycle in phase with summer rainfall, and show a strong and rapid response to large rain events (**Figure *3***b). The period of large events since 2015 has increased the total vegetation and SWE extent in the basin to the highest levels since at least the 1980s.

Streamflow in the Rio San Pedro shows a clear response to large precipitation events, particularly in 2001 (a maximum of 13 m^3/s in March) and 2012 (**Figure *3***c). This strong response likely reflects the efficient channeling of runoff in this large perennial river during these events. These rapid responses are superimposed on a relatively small but consistent annual signal of higher flows in the winter when evaporation is low and a consistent decreasing trend throughout the record. A seasonal Mann-Kendall test of monthly average discharge in the river recorded from 1984 to 2015 shows a statistically significant decreasing trend (p-value = 7.57E-09) amounting to a total decrease in monthly streamflow of 0.01 m^3/s. Changes in TWSA from GRACE show a period of relatively low storage during the Mega Drought and a strong increasing trend since then (**Figure *3***d). Since this drought also happens to coincide with the baseline period over which the anomaly is determined, we cannot directly quantify the effect this drought had on storage volumes relative to the period before. However, we can observe that there was less total water stored in the basin during the drought than there was following the large events in 2012 and especially during the wetter period that followed. Since the end of the Mega Drought, terrestrial water storage in SdA has increased by a basin-wide equivalent thickness of 3-10 cm. The clear annual signal in these data, like vegetation extent, is in phase with summer precipitation and responds strongly and rapidly to large precipitation events while also showing rapid declines during years with low rainfall. As Ahamed et al. (2021) show, GRACE is quite effective at capturing responses to large recharge events. The similar response in vegetation and water storage in the basin may reflect that these systems are primarily responding to changes in shallow vadose zone soil moisture.

4.2. Water Use and Lithium

We present the first basin-wide assessment of allocated and actual freshwater use for SdA. **Figure 4**a shows the spatial distribution of water concessions scaled by permitted extraction allowances. We further differentiate and aggregate these data by water use type for both allocated (**Figure 4**c) and estimated actual use (**Figure 4**d). A review of the national database performed in cooperation with local parties yielded several observations about these allocations. Most of the water use permits are allocated to copper ("other mining") and agriculture, which claim 47% and 34% of total water rights. The third and fourth highest allocations are lithium and potash mining companies with 10% and "other" uses with 7%.

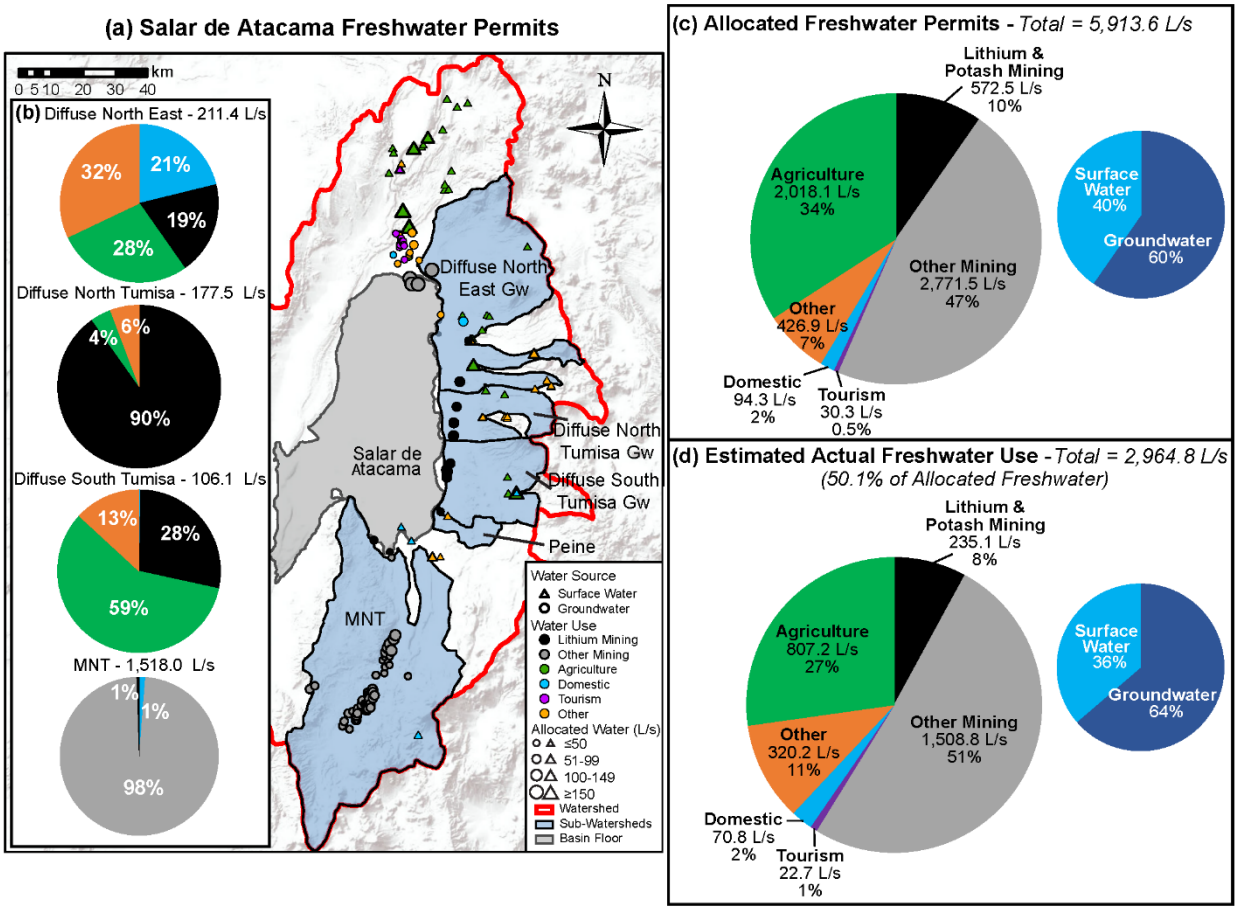

Figure 4. Freshwater allocation and use in the SdA basin. With **(a)** allocated freshwater permits divided by water source (symbol shape), use category (symbol color), and allocated amount (symbol size). **(b)** Pie charts of estimated actual freshwater use in 2014 within each sub-watershed zone divided by use category - lithium mining (black), other mining (grey), agriculture (green), domestic (blue), tourism (purple), and other (orange). No withdrawals occur within the Peine sub-watershed zone. Pie charts in **(c)** and **(d)** represent total allocated freshwater permits and estimated actual freshwater use in 2014, respectively.

Domestic uses make up 2% of total allocations, and water extraction that is strictly relevant to the tourism industry comprises the remaining 0.5%.

Besides other mining extraction, agriculture is the second largest use type by category and therefore we note the relative spatial disruption of agriculture versus mining in the basin. First, most of the agricultural consumption is located upgradient of fresh groundwater extraction for lithium and potash mining purposes (**Figure 4**). Second, agricultural freshwater consumption consists primarily of surface water from streams located along the northern and eastern slopes of the basin. Finally, it is important to note that the understanding of actual consumption is limited to reported pumping rates from industrial users and poorly constrained estimates based on hydrologic observations for non-industrial users. Therefore, there is substantial uncertainty in the estimated freshwater use for agricultural purposes. Yet the estimates used in this study are conservative considering the relative basin-wide impacts of agriculture on freshwater consumption.

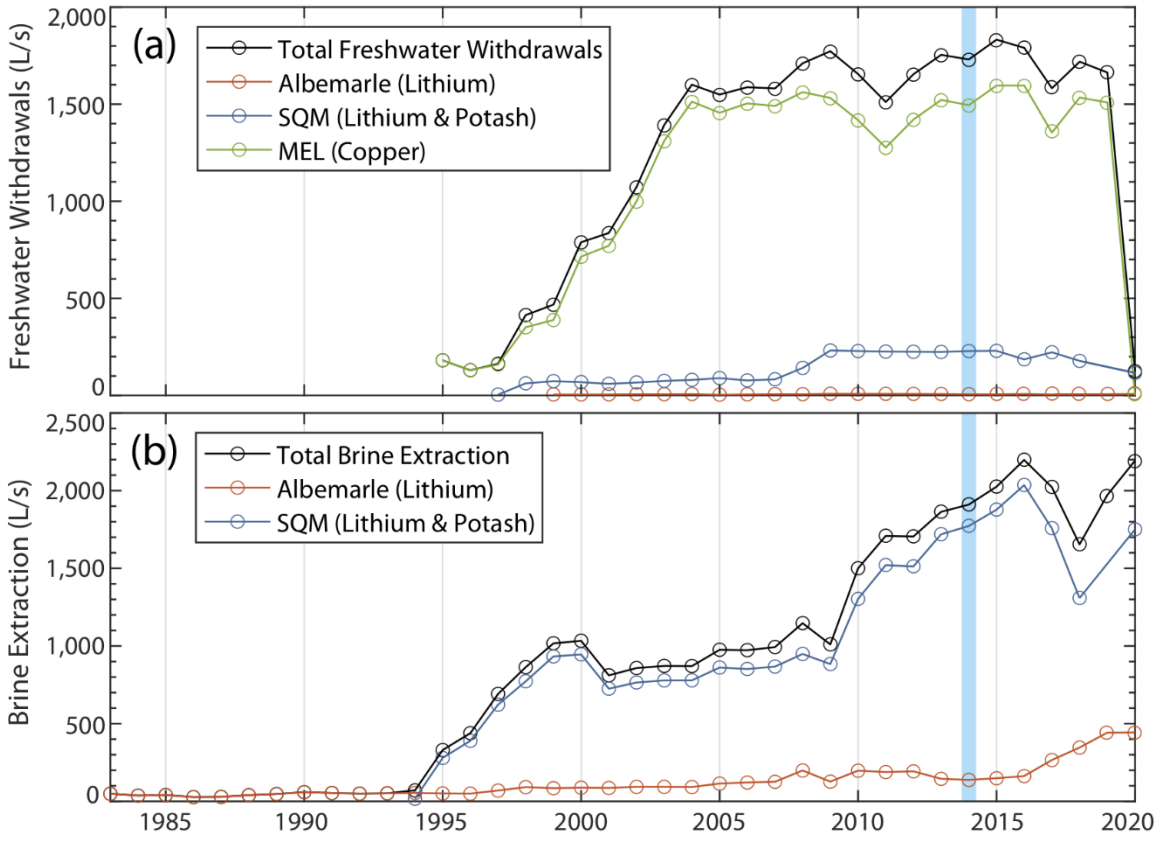

Figure 5. Annual freshwater **(a)** and brine **(b)** withdrawals associated with mining operations in the SdA basin. Minera Escondida Limitada extractions from ended in 2020. The blue bar represents the time frame (2014) of the water use assessment presented in **Figure 4**d.

Our findings illustrate that publicly available water extraction amounts do not equal actual extraction in the basin. While several public reports have collated anthropogenic extraction limits based on government-issued water use permits, we find that actual water use has historically been monitored for industrial users and virtually unmonitored for private, non-industrial users (AMPHOS21, 2018). **Figure 5** presents the history of both brine and freshwater extraction within the basin. Freshwater extraction (**Figure 5**a) is separated by user to show the relative contributions to total lithium and potash and other mining withdrawals in **Figure 4**d. Specifically for lithium & potash mining, freshwater extraction is approximately 41% of allocated water (i.e., 235.1 of 572.5 L/s), with Albemarle Corporation consuming 6.5 L/s and SQM using 228.6 L/s in 2014 (blue bar in **Figure 5**). Thus, freshwater extraction for lithium mining purposes equates to approximately 8% of total actual freshwater extraction for the basin. Actual water use is further divided by sub-watershed zone to illustrate its spatial distribution and potential impacts (**Figure 4**b). Most actual withdrawals (1,518.0 L/s) are from the MNT zone. Diffuse North East, Diffuse North Tumisa, Diffuse South Tumisa, and Peine represent 211.4, 177.5, 106.1, and 0.0 L/s, respectively. A comparison between actual freshwater use in 2014 and 2020 are included in the supplemental material (**Figure S2**).

4.3. Relic/Modern Water

Inflows to the SdA hydrological system can be divided into three unique water compartments or sources defined by their flow paths and mean transit times. This refined understanding builds upon previous works by Jordan et al. (2002), Houston and Hart (2004), Rissmann et al. (2015), Corenthal et al. (2016), Boutt et al. (2016), Moran et al. (2019), and Munk et al. (2021). These sources are: i) direct precipitation and runoff (most of which does not become groundwater recharge except perhaps within the salar nucleus) with short mean transit times and residence in the system (weeks to months), most of this water leaves the basin as soil or open water evaporation near the salar floor; ii) groundwater inflow from the large and deep regional groundwater system which constitutes baseflow to springs and streams and the majority of total inflow to the basin, these waters have long mean residence times (>>65 years) and are largely decoupled from the influence of modern climate; and iii) local, intermediate groundwaters with mean transit times on the order of 1-10 years, sourced predominantly from local modern recharge within the high-infiltration capacity alluvial aquifers along the margin of

474 the basin floor. This third water source also likely contains large contributions of water from ^{3}H-
475 dead stream water and springs and runoff from large rain events re-infiltrating along preferential
476 pathways in the alluvium, therefore, its age distribution is likely highly spatially variable. We
477 define the distribution of these three general water sources, their contributions to the

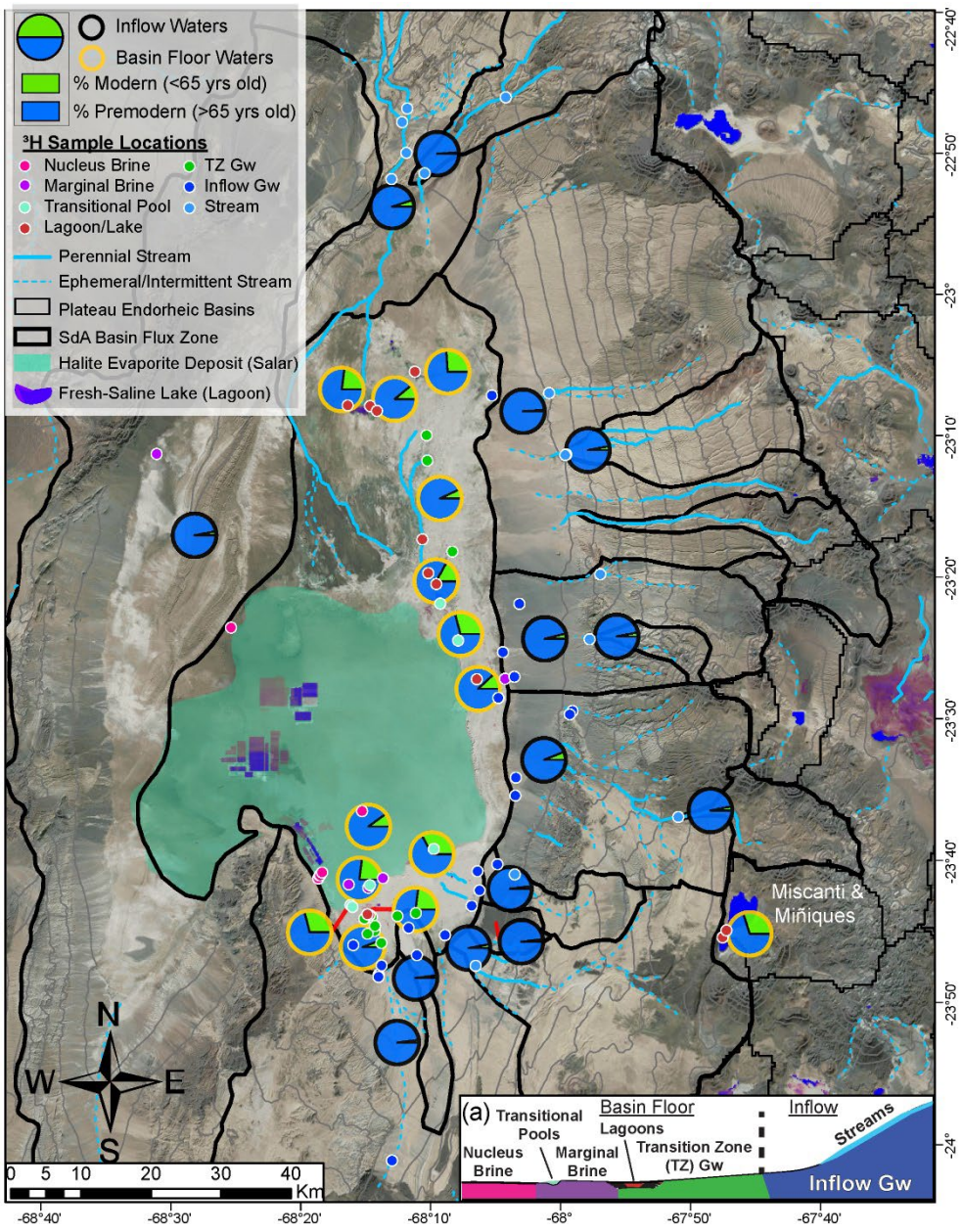

Figure 6. Distribution of modern/premodern (relic) water content. Pie charts show this ratio grouped by inflow zone (black outline) which includes springs, streams, and groundwaters, and basin floor water bodies (yellow outline). The high elevation lakes Miscanti & Miñiques outside the topographic watershed are included. Black lines delineate zones of flux into the basin and the approximate outline of the basin floor (as defined by Munk et al., 2018). Light grey lines are 250-meter contours of elevation. Colored dots show all samples collected for this work classified by water type (n=106). **(a)** Inset cross-sectional schematic defining the physical water body classifications.

hydrological budget, and their contributions to specific surface and groundwater bodies using ^{3}H as a relative age tracer combined with other geochemical signatures.

We define the relative age of all surface and groundwater bodies within the SdA basin using a large, comprehensive dataset collected over 10 years (**Figure *6***). Our results show consistently low modern water content among inflow waters feeding the basin floor including all streams, springs, and groundwater. Values range from 0% to 7% among 45 samples. One additional sample is a notable outlier, containing 15% modern water, due to its location in an alluvial fan near the salar margin at ~10 mbgl it may represent a local groundwater flow path described above. By partitioning all basin inflows into sub-watersheds where the relative flux was quantified by Munk et al. (2018) we show that most of the flux to the basin (57%) contains very little modern water content (≤4%), another 12% of flux contains an average of 6% modern water but is skewed by the one outlier sample noted above. The final 31% of influx to the basin comes from the San Pedro River in the north with 5% modern water content. This river, considering its large contribution to total inflow may act to transport small but focused amounts of modern water to the basin floor. However, our results show that most of the inflow water volume to the basin is composed of waters with essentially no modern content. Another important result, which is apparent in **Figure *6*** is the strong and consistent difference in modern water content between the inflow waters and surface and groundwaters on the basin floor.

In contrast to the inflows, all water bodies on the basin floor (defined in **Figure *6***a) contain a substantial proportion of modern water. The Transition Zone Groundwaters average only 6% modern but range between 0% and 21% illustrating its position at the interface between the basin inflows and the salar floor water bodies (the full statistical distribution of these water bodies is shown in **Figure 7**a). In surface water bodies at the salar surface, the Lagoon waters range between 8% and 28% and Transitional Pool waters between 16% and 53% indicating a strong influence of modern inputs, strongest in the latter. As a point of reference, samples from a pair of high elevation lakes near the watershed divide average about 30% modern, illustrating that high modern water content in surface water bodies in this region is not unique to the SdA basin floor. In the brine aquifers, the Marginal Brine contains between 2% and 36% modern, and the Nucleus Brine contains between 2% and 20%. The presence of both ^{3}H-dead and high modern content waters suggests that these brine aquifers receive inflow from multiple

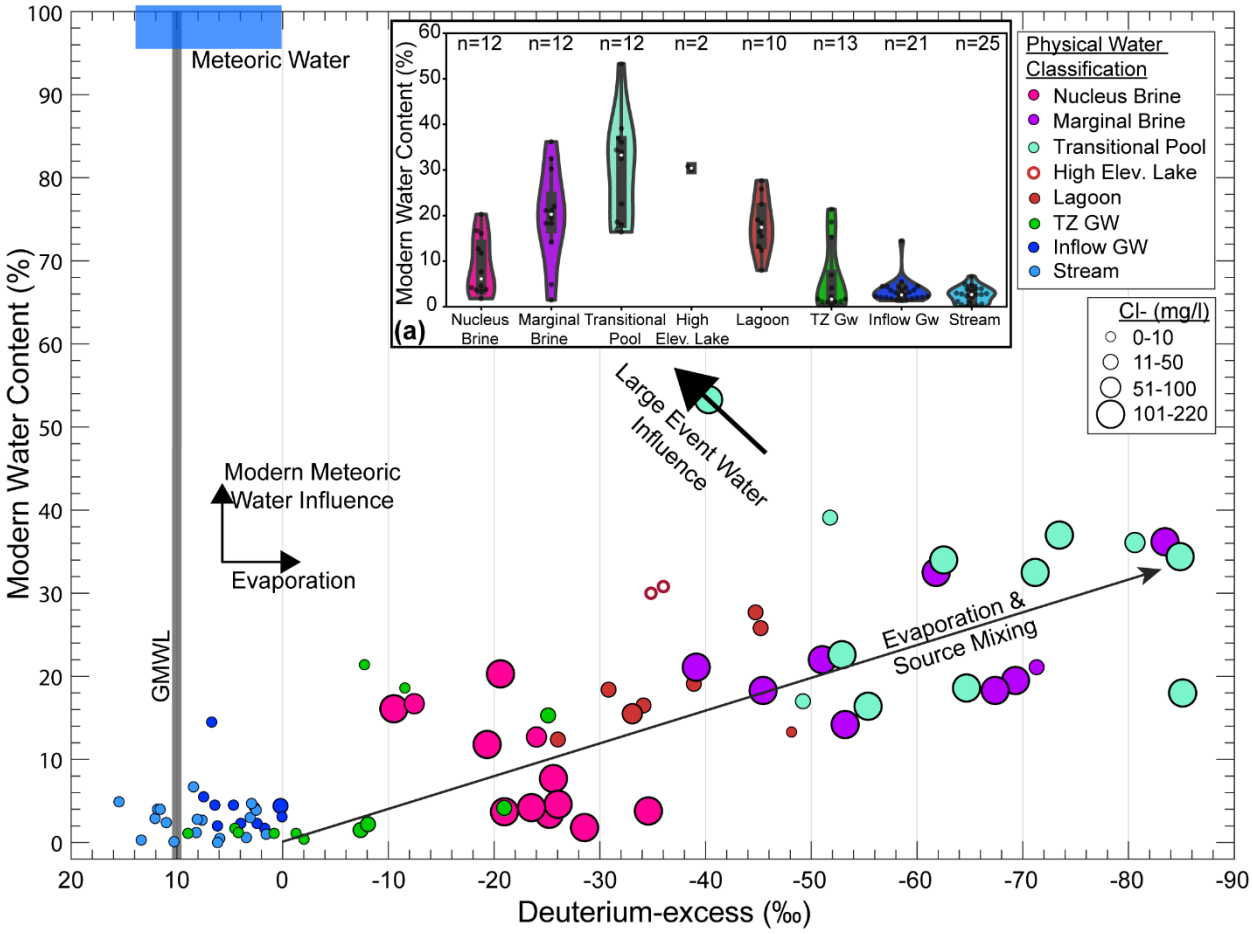

Figure 7. Processes controlling physical water distinctions and interactions. Circles are proportional to chloride concentration in each sample. The grey vertical bar is the Global Meteoric Water Line (GMWL), and the blue box represents the approximate range of meteoric input waters (based on Moran et al., 2019 data). Arrows depict the influence of important hydrological processes and interactions. **(a)** Violin plot of all data grouped by physical water type. Grey boxes show the interquartile range; white dots are the median and the colored polygons represent the frequency distribution of the data (black dots).

compartmentalized sources. The compartmentalization of water bodies and their interactions in the SdA system is illustrated in **Figure 7**.

The relationship between relative water age and deuterium-excess as well as Cl^- concentrations in sampled waters allows for the differentiation of distinct water bodies based on their dominant source and degree of interaction with the atmosphere. This interaction in this very arid environment imprints a strong evaporative signature on the stable H and O isotopes in water, resulting in increasing negative deuterium excess. Important results here include the strong differentiation of inflow waters from the brines and surface waters on the basin floor. This consistent signature suggests these inflow waters have been segregated from the atmosphere over

their entire transit, as there is no evidence of evaporation. These waters are sourced from relic recharge, nearly all their volume is water that entered the ground at least 65 years ago. In contrast to these waters, the surface water bodies and brines show both a strong signal of evaporation and a higher proportion of modern water. The Transitional Pools have the highest median percent modern value and the strongest evaporative signature (**Figure 7**a) likely reflecting that their primary source is large modern rain events that flood the margin of the salar, then rapidly evaporate and become saline. The Marginal Brines interestingly have a quite similar signature to these surface waters suggesting a proportion of these waters share a similar source. Brines contained within the nucleus aquifer are quite distinct from both the inflow and the marginal brine and surface waters indicating inputs from several sources that may be somewhat compartmentalized, some from mixtures containing mostly relic but evaporated water, and some from a source containing more modern but less evaporated water. The Lagoon waters and Transition Zone Gw results indicate they are likely sourced by a combination of relic inflow water and modern rainwater. Lagoon waters contain high modern content and strong evaporation signatures but are also fresher than the Brines and Transitional Pools. The shallow groundwaters in the transition zone on the other hand are quite variable, some appear very similar to the old, fresh inflow waters and some more similar to the Nucleus Brine and Lagoon waters. This likely reflects the fact that they are at the interface between the regional inflow and basin floor, so they are fed by inflow waters but also by modern meteoric waters that feed the surface waters near the basin floor. These results again reiterate that the basin water budget is dominated by regional inflow waters but also that critical insight can be gained by understanding the distinct sources in the system.

The modern/premodern (relic) water ratios presented here are relative values based on the estimated input activity of precipitation and surface and groundwater samples whose value represents an unknown distribution of ages. Therefore, to better contextualize these values within a physical framework we use a simple piston flow transit model to predict modern water content at sample sites based on logical physical properties. This allows for a direct comparison between our observations of water age from the field and those predicted within a strictly physical framework. This model is highly conservative, intentionally reducing assumptions as much as possible, and utilizes parameters from a simple model in a similar arid environment presented by Houston (2007). We calculated the distance and gradient from the watershed divide directly

548 upgradient of 16 sampled inflow waters dispersed along the basin margin and applied a range of
549 physical properties to estimate seepage velocities and transit times between the recharge area and
550 sample site. Assuming recharge waters have a ^{3}H activity equal to that of modern meteoric
551 water, we decayed that input over the transit time to the discharge point. As described above, we
552 know that most of the inflow to the basin is groundwater so we (conservatively) assume that
553 water emerging at the sample site will be a mixture of 2/3 this decayed recharge water and 1/3
554 meteoric water that has been decayed one year to represent recent recharge infiltrating and
555 mixing with these waters. The activity in this mixture is the model-predicted activity of water
556 emerging from the ground at the sample site. Comparing the water composition predicted by this
557 model using a range of plausible hydraulic conductivities and our measurements in the field, the
558 physically-based model consistently predicts percent modern water content in inflow waters
559 greater than an order of magnitude higher than we observe (**Figure 8**). Again, this model is
560 highly conservative and not designed to directly model the flow of regional groundwater in the
561 basin, but it serves to illustrate that the assumption of springs, groundwater, and streams, which
562 are essentially ^{3}H-dead, as sourced from recharge entering and discharging the basin on modern

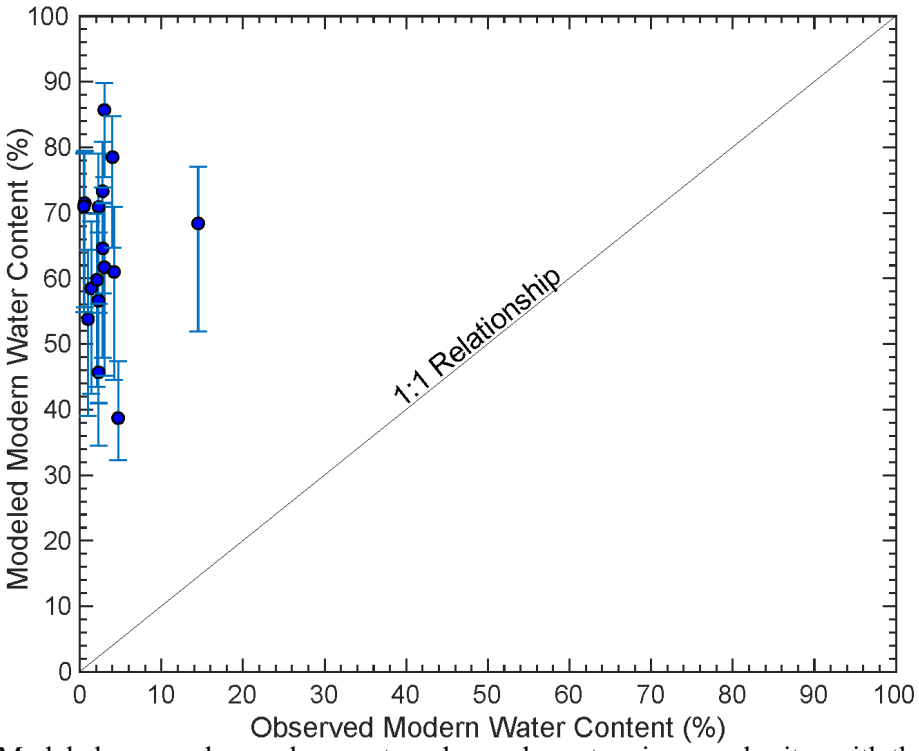

Figure 8. Modeled versus observed percent modern values at major sample sites with the line of direct 1:1 relationship. Modeled values are based on the piston flow transit model described in section 4.2. Blue dots are modeled values (K = 10 m/d), high-low range represented by K=15.5 m/d and K= 5 m/d respectively.

time scales cannot be reconciled with observations. The discrepancy between observed and modeled values also highlights that the existing conceptual models of this system, at modern hydrological balance are not capturing the fundamental hydrological dynamics required to adequately constrain the water budget. A complete description of the data and calculations for this model are presented in **Table S2**.

4.4. Water Budget with Relic Water

To illustrate the meaning of our findings we compare the existing conceptualization of the SdA water budget used by the DGA to manage water use in the basin (DGA, 2013) to a revised conceptualization that incorporates our understanding of water fluxes and sources (Boutt et al., 2021). These conceptualizations are summarized in a Sankey diagram (**Figure 9**) that

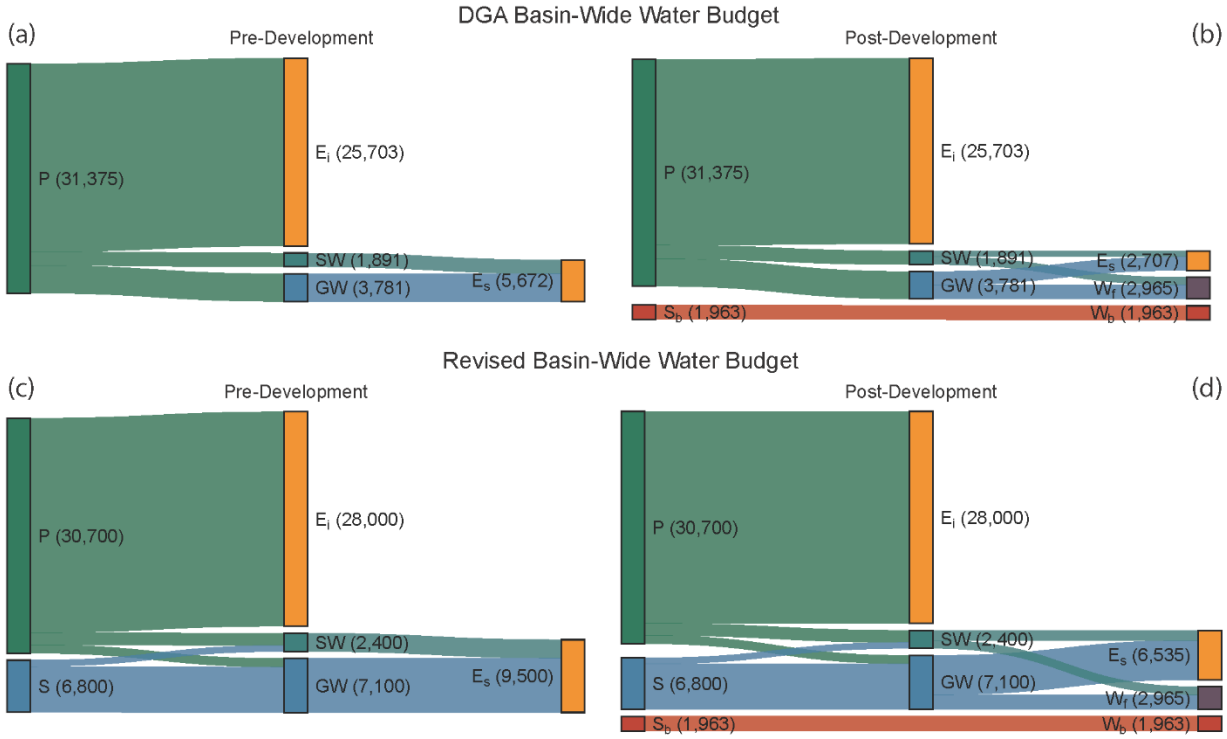

Figure 9. Current (DGA) and revised conceptualizations of the SdA basin water budget. Sources of water are on the left side of the Sankey diagrams and sinks are on the right. All terms represent water or brine flux in units of L/s. Precipitation (P) becomes infiltration losses due to evaporation (Ei) or the modern recharge component to surface water (SW) and groundwater (GW). **(a)** Current DGA conceptualization of the water budget without anthropogenic withdrawals with all SW and GW flux resulting in evaporation on or near the salar floor (Es). **(b)** Current DGA conceptualization of the water budget with anthropogenic water withdrawals (Wf) and brine withdrawals (Wb) from storage in the brine body (Sb). **(c)** Revised conceptualization of the water budget with additional groundwater flux from storage (S). **(d)** Revised conceptualization of the water budget including anthropogenic withdrawals.

shows the pre-development understanding of the water budget (**Figure 9**a,c) and the impacts that anthropogenic water use would have on the water budget (**Figure 9**b,d). Details of the data and calculations are provided in the supplemental information (**Text S2**).

The DGA conceptualization (DGA, 2013) presented in **Figure 9**a assumes that the system is at a steady-state within the topographic watershed. With this assumption, the modern recharge, which is the sum of precipitation flux (P) to surface water (SW) and groundwater (GW), balances all evapotranspiration from the salar (E_s) with no net storage flux (S). As presented above, the assumption that all flux comes from modern recharge and flows along intra-basin flow paths (<50 km) to the basin floor is not supported by our relative water age observations. Also, based on this conceptualization, the net basin yield is 18% of P, a number that is extremely large for arid watersheds even when accounting for infiltration from large and infrequent precipitation events (Scanlon et al., 2006; Houston, 2009; Boutt et al., 2021).

We then apply anthropogenic freshwater (W_f) and brine (W_b) withdrawal estimates for the basin to the DGA conceptualization of the water budget (Figure 9b), assuming that all W_b flux results in a corresponding net storage flux from the brine body (S_b). We find that W_f results in a 48% reduction in E_s to maintain the hydrologic balance within the steady-state assumption. A portion of E_s includes the environmental flow requirement for sensitive wetland ecosystems along the salar margin. Although the effects of a reduction in E_s on environmental flows are not evaluated here, we assume that a reduction in E_s should result in some reduction in environmental flows.

The revised conceptualization presented in **Figure 9**c does not assume steady-state conditions within the topographic watershed and instead is based on flux estimate data from 1998 to 2009 (Boutt et al., 2021). The modern recharge estimate of 2,700 L/s (1,600 L/s to SW and 1,100 L/s to GW) results in a net basin yield of 9%, which is significantly lower than the DGA conceptualization. In this conceptualization, the majority (86%) of GW flux comes from S, which includes both pluvial groundwater storage within the basin from wetter past climate regimes as well as long groundwater flow paths from outside of the topographic watershed (Corenthal et al., 2016; Boutt et al., 2021), both of which are supported by our relative age observations. **Figure 9**d applies the W_f and W_b estimates to the revised conceptualization with the same assumptions applied to S_b and E_s. This results in a 31% reduction in Es to maintain the hydrologic balance.

The revised conceptualization shows that by overestimating modern recharge and net basin yield, the DGA conceptualization underestimates groundwater storage losses and overestimates the relative change in E_s. Moreover, reductions in precipitation due to recent droughts will manifest differently depending on the conceptualization of the water budget. The reduction in modern recharge due to decreased precipitation during the recent drought periods, although not directly quantified here, would have a larger impact on SW and GW flux under the DGA conceptualization compared to the revised conceptualization.

5. Discussion

5.1. Importance of groundwater residence time and natural variations to ground-truthing hydrological interpretations

Although the SdA hydrological system is controlled by regional groundwater draining from storage, disconnected from the modern climate, short-term climate variations (droughts and large rain events) significantly impact surface water bodies and soil moisture in the basin. In addition, major droughts reduced SWE and vegetation extent while at the same time mining-related water extractions (from lithium and copper) dramatically increased. Wet intervals and extreme precipitation events during this period also had strong and rapid effects on the wetlands and surface water bodies in the basin. Despite ongoing brine and freshwater extractions, multiple extreme rain events since 2015 have increased SWE and vegetation extents overall, and total terrestrial water storage has also increased substantially (**Figure 3**d), likely due to large pulses of recharge from these extreme rain events making their way through thick vadose zones above the regional groundwater table. These results highlight the important role that climate variations have on the water budget irrespective of anthropogenic influence. Any analysis of hydrological impacts in arid regions such as this must disentangle these climate variations from anthropogenic effects.

As global climate change becomes increasingly apparent, assessing impacts in SdA in the context of these changes will become even more important. Indeed, a recent study found that mean annual temperatures have already increased by >0.5°C over large parts of the dry Andes since the 1980s (Frau et al., 2021). The most recent projections of climate change in this region over the next several decades show that average temperatures will continue to increase (by 2-5°C

633 by 2100), the duration of seasonal snow and ice cover will decrease (by ~30 days by 2100), and
634 though projections for precipitation range anywhere from a slight decrease to a slight increase
635 overall, the timing of rain events is likely to change and the intensity increase (Pabón-Caicedo et
636 al., 2020; Bambach et al., 2021). Recent work shows the potential for increasing overall moisture
637 supply and large precipitation events in this region due to a southward shift in the South
638 American Monsoon and available moisture from the Amazon (Jordan et al., 2019;
639 Langenbrunner et al., 2019; Pascale et al., 2019). The most recent period of extreme events
640 (2015-present) may be a direct reflection of these climate changes, and therefore these events
641 may become more frequent. As we have outlined in this work, these extreme events have a major
642 impact on the surface water and wetland systems of SdA.

643 Though it may seem intuitive to attribute periods of decline in surface waters, wetland
644 vegetation, and groundwater levels at the margin of the salar to intensive, industrial-scale
645 extraction of lithium-rich brine and fresh groundwater in a very dry environment, the framework
646 we describe here shows how climate variability confounds this attribution. Correlation does not
647 equal causation, and for the reasons outlined in this work, great care must be taken when
648 attributing causes to specific impacts. For instance, the Rio San Pedro, which is isolated from
649 any potential impacts from the long legacy of water extraction for mining operations, shows a
650 steady and statistically significant decline in discharge since the 1980s (**Figure 3**c). The
651 watershed of this river is large and likely receives water from a combination of the three sources
652 of inflow outlined in section 4.3. Although ^{3}H results show that most of its flow originates from
653 relic groundwater, decreases in shorter-term inputs, due to accumulated precipitation deficits
654 from two long-term droughts may contribute to a decline in overall flow over decadal time
655 scales. In addition, it is difficult to quantify the impacts of water use changes at the many
656 agricultural plots in the watershed (**Figure 4**a), which may also contribute to the decrease in
657 discharge from the largest river in the basin.

658 Freshwater use for lithium and potash mining has had a small impact compared to copper
659 mining and other water uses. Groundwater storage declines have occurred throughout the basin
660 but are most pronounced in the MNT aquifer, where copper mining groundwater extractions are
661 concentrated, and in the Diffuse North East sub-watershed zone, where the primary water users
662 are other uses, agriculture, and domestic (**Figure S3** and **Figure 4**a). Of the fresh groundwater

zones where anthropogenic extraction occurs, the two sub-watershed zones where lithium and potash mining extractions are the most concentrated (Diffuse North Tumisa and Diffuse South Tumisa) experienced the smallest groundwater storage declines. Focusing water conservation efforts on the water users in the MNT aquifer and the Diffuse North East sub-watershed zone would have the greatest impact in minimizing harm from the overallocation of water rights in the basin.

As we have described here, surface waters and vegetated wetlands are supported in large part by baseflows into shallow water tables from regional groundwater discharge but are also quite sensitive to changes in modern precipitation. Declines in regional groundwater inflow have major and lasting impacts on these systems; however, these effects can be offset at least at the basin scale by increases in precipitation related to natural climate variations. Impact assessments on local wetlands must account for both processes.

5.2. Allocation of water rights and implications of brine extraction under an inadequate hydrological understanding

Current water allocations in SdA are based on an inadequate hydrological representation of the system and as a result, are substantially greater than what can be replenished on modern time scales. Most water currently being used is not derived from modern rainfall, but relic groundwater stored in local and regional aquifers; this water may be a “sustainable” source of water, but specific thresholds for extraction of these old waters must be determined. What constitutes sustainable extraction depends heavily on the location of extraction as freshwater aquifer extractions have larger and more rapid wetland impact potential than brine aquifer extractions. Responsible water allocation must incorporate this important fact. As outlined in this study, current conceptualizations of the source and residence time of waters being extracted are inadequate, and therefore truly sustainable water use metrics have likely never been met.

There are a few key implications of this misallocation of water in the basin. The assumption underlying current water allowances is that water use is sustainable or renewable if total withdrawals do not exceed inflows from modern recharge within the topographic watershed and runoff minus evaporative losses. Most of the groundwater entering the basin is, in fact, decoupled from modern recharge and therefore is not being replenished on human time scales.

Allocation of this groundwater under the assumption that it is immediately replenished is the primary reason that water has been overallocated. The impacts of this inaccurate assumption are likely localized to areas near actual extraction. For instance, the large amounts of water allocated to copper miners in the upper part of the MNT aquifer would be entirely sustainable if the DGA water budget conceptualization was correct. However, as we have shown here, the concentrated use of this water over several decades has led to drawdowns in the aquifer significantly greater than other aquifers in the basin (**Figure S3**), indicating that this water use is not sustainable. This aquifer drawdown may impact wetlands fed by this water. Sustainable metrics must be determined based on the source and residence time of the specific waters being extracted, not basin-wide inflow estimates within a steady-state water budget.

Not all water extraction is equal in the basin as illustrated by the strongly discretized compartments in **Figure 7**. The impacts from brine extraction cannot be equated to the impacts from fresh groundwater extraction. As shown here and in previous works (e.g., Munk et al., 2021), the brines being extracted for lithium are hosted in aquifers that are disconnected (on human time scales) from surface water and wetland systems at the margin of the salar while regional groundwater inflows provide critical baseflows that maintain these systems. In 2014, lithium mining made up only ~8% of total freshwater extraction in the basin whereas copper mining made up ~51%, these values are representative of the approximate average annual extraction rate over the past decade. Though the copper mines have ceased freshwater withdrawals as of 2020 (**Figure 5**a), due to long response times in these systems, the impact from two decades of intensive extraction will likely continue for some time. Although the lithium mines are located much closer to sensitive wetland systems, the actual impacts from their water use are significantly less than that of copper mining, corresponding to relative extraction volumes from the same inflow waters. Therefore, water allocations must be adjusted within this revised conceptual understanding if they are to meet and maintain truly sustainable metrics while preventing local impacts to surface and groundwaters.

5.3. Problems associated with prior assessments of water storage and NDVI changes in the basin

The environmental impacts of lithium brine mining necessitate investigation, yet several scientific publications that address the subject assume environmental impacts based on conceptualizations that are both dissonant with the current understanding of the hydrological dynamics of the basin and inconsistent with data-based observations. One example is Liu et al. (2019), which attempts to directly correlate environmental degradation with areal mining growth using several remote sensing products from JRC and MODIS. While using the NDVI product from MODIS as a key metric in this study, the authors attribute the full range of NDVI (-1 to 1) as directly proportional to green vegetation loss whereas published applications of NDVI apply thresholds to specific ranges for vegetation identification and differentiation. The authors' approach is neither justified in the manuscript nor proven in previous studies and is discordant with our analysis using NDVI within previously defined ranges to identify areas of vegetation, which indicates that vegetated area has increased through the past decade (**Figure *3*b**). A further confounding issue is the inclusion of the built evaporation ponds in their NDVI assessment, water bodies result in negative values in the index and thus would bias NDVI towards more negative numbers. Their conclusion of expanding degradation is increasingly implausible when considering that it has no grounding in the basin's hydrology; precipitation has increased over recent years following the extreme drought and spring and surface water recharge is dominated by relic water.

Another recent publication by Liu & Agusdinata (2020) argues that extraction of brine in SdA over the last few decades has led directly to a decline in terrestrial water storage in the basin, directly contradicting the results presented in this work (**Figure *3*d**). Using GRACE TWSA, they argue that between 2002 and 2017 water storage in the SdA basin declined at a rate of 1.16 mm/year; however, the method presented to extract, process, analyze and interpret these data is fundamentally flawed for several reasons. The source of data is a pre-processed GRACE dataset hosted by the University of Colorado Boulder (http://geoid.colorado.edu/grace/index.html), but the authors do not adequately describe the processing performed to justify their results, making their results not reproducible. The domain over which their analysis was conducted is not clearly defined, and the authors do not justify why the region

assessed is appropriate to reach their conclusions about SdA. The USGS Level 2 river basin boundary (described as the domain of their analysis) encompasses an area much larger than the SdA basin, including a large portion of the hyper-arid Atacama Desert and the Pacific coast, >100km to the west of the SdA watershed. They assume that trends observed over this much larger domain reflect changes in water storage in the SdA basin without providing supporting evidence. The dataset used for their results utilizes a land surface-hydrological model (GLDAS-CLM Hydrology) as a gain factor to scale the filtered GRACE data. However, an independent assessment of this model within the SdA basin showed a strong increasing trend in storage, opposite to that presented by the authors (**Figure S4**). As described in Landerer & Swenson (2012), the gain factors derived from the model outputs used to scale the GRACE data are intended to reduce small errors in the GRACE data from signal modification (e.g., attenuation). In this case, the scaling has reversed the resulting trend, not merely reduced small errors. Even if the negative trend they describe is to be believed, the magnitude of change is very small (1.16 mm/year) and given that the magnitude of storage changes observed by GRACE and that the uncertainty associated with those data are at centimeter-scale, this trend could be within the margin of error of the dataset. There is no explanation of whether this trend is statistically significant and no assessment of error. In addition to SdA, our independent analysis of GLDAS also found a positive trend in the Atacama region within their domain, leading us to conclude that this major discrepancy likely results from known issues with using GRACE data and model scaling factors for near-coastal regions (Wiese et al., 2016). These issues in addition to the fact that an assessment of GRACE within the SdA basin by Montecino et al. (2016) and our analysis of the SdA basin show a strong increase in total TWSA over the same period of ~5 cm (**Figure *3*d**), illustrates serious flaws in the analysis by Liu and Agusdinata (2020). The lack of confidence in the validity of these results discredits any conclusions reached therein about water availability changes at SdA.

5.4. Global implications of approach and results

This work constitutes a comprehensive assessment of the SdA hydrological system specifically; however, this work has both regional and global implications regarding the assessment of water resource sustainability in drylands. First, the Mega Drought we've identified at SdA is part of a continental-scale phenomenon that is one of the longest and most severe

droughts of the past millennium in this region (Morales et al., 2020, Garreaud et al., 2020). The region hosts dozens of salar systems that display a similar set of climatic and hydrogeologic conditions that manifest in similar fundamental hydrological controls (Moran, 2022). The responses to anthropogenic and natural changes we document at SdA can therefore be directly applied to understand these environmental impacts in basins across the region. This drought has also been directly tied to the similarly anomalous Mega Drought currently occurring in the western United States, both are likely triggered or greatly exacerbated by global climate change (Steiger et al., 2021; Garreaud et al., 2021). The western US also contains many lithium-bearing salars currently being explored for development, the water resources in these arid basins can also benefit greatly from an improved understanding of these systems. The method we've applied to document and interpret hydrological changes and responses in these environments addresses key issues of water, human well-being, ecosystems, and climate in connection with global resource and energy needs critical to our common future. Our findings make key advancements in our understanding of natural water cycles in arid regions, current and future impacts from global climate change, and new insights into the unique and elusive features of brine groundwater hydrology.

6. Conclusions

Utilizing lithium brine and freshwater resources in arid basins while effectively mitigating impacts from its extraction is unattainable without a comprehensive science-based understanding of these hydrological and geochemical systems. Our approach is the most rigorous and complete hydrological assessment of the SdA basin to date, outlining persistent shortcomings in current water allocations and evaluation of impacts. We outline a method to address these issues in the SdA basin that can be directly applied to the many arid endorheic basins globally with significant current or future water demands. Our analysis shows that climatological variations at SdA have caused major natural changes in surface water and vegetation extent, streamflow, and basin-scale water storage on annual and decadal scales. Anthropogenic water extraction has had important localized impacts on surface and groundwaters, which are discussed here, but these changes can only be attributed after accounting for the influence of natural variation. Relative extraction by different users must also be considered when attributing impacts, especially with freshwater extraction which has a much

larger impact on wetlands, lagoons, and freshwater resources than brine extraction. The largest freshwater users in the basin have been copper mining and agriculture, and the largest groundwater storage losses have occurred where these two users are concentrated.

In addition, we show that the current SdA water budget is based on an outdated and inadequate understanding of fundamental hydrological processes making it insufficient to allocate water rights at sustainable extraction rates. We document that most of the current inflow to the basin was recharged before the modern climate regime; therefore allocating water rights based on an assumption of a system in steady-state with the modern climate is inherently flawed. The considerable overallocation of water in the basin sub-catchments over the past few decades has stemmed primarily from assumptions that overestimate water resource sustainability, illustrated in our revised water budget. Future work on the water budget of SdA (and other arid lithium-bearing basins) must recognize and explain the role of relic groundwater in the water budget and explicitly incorporate geochemical tracer data into physical hydrologic models. Furthermore, our new conceptual framework highlights the need to assess water extraction rates in the context of sources of the water being extracted since responses to perturbations (natural or anthropogenic) can be very different depending on where extraction is occurring (i.e., brine aquifers vs fresh marginal aquifers). This work has far-reaching implications for future water management and mitigation of impacts in the SdA basin and is an effective guide to sustainably utilize water and brine resources globally.

Acknowledgments

The authors would like to thank BMW Group and BASF SE for funding and supporting this research. We also want to thank Ricki Sheldon and the Council of Peoples Atacameños for graciously volunteering to conduct a sampling campaign that was pivotal to this study. In addition, we would like to thank Dr. Matt Winnick and Dr. Justin Richardson for access to their analytical geochemistry instruments and equipment, and Alex Grant for valuable perspective and feedback on this manuscript. There are no real or perceived financial conflicts of interest for any of the authors.

Open Research

Raw data used to produce the remote sensing results presented in section 4.1, and all data included in the supplementary information are compiled in an open access data repository for this work (https://doi.org/10.7275/e7t9-ta95).

Figure Captions:

Figure 1. Major lithium-bearing basins of the Dry Andean Plateau of South America. (a) The regional mean annual precipitation of the region and the SdA basin topographic watershed are outlined in red. (b) Inset map of the SdA basin and its hydrological features. The salar nucleus, transition zone, surface waters, vegetated wetlands, and perennial streams are outlined. Meteorological stations and the stream gauge are labeled along with the location of fresh groundwater extraction wells. The MNT aquifer is highlighted in green, and streams (rivers) are in blue.

Figure 2. Annual precipitation from 1984-2020. Vertical red/blue bars represent major climate intervals identified. (a) Shows records from meteorological stations within the basin, the Rio Grande station record is a dotted line due to its location at the northern end of the basin. (b) The basin-wide area-integrated annual precipitation from the TerraClimate dataset with the 3-year moving average. The Mean Annual Precipitation (MAP) from the TerraClimate record (1958-present) is indicated by the blue horizontal line.

Figure 3. Changes in basin-wide hydrological conditions since 1985. (a) Total monthly surface water extent and TerraClimate total monthly precipitation, (b) total monthly extent of living vegetation, (c) average monthly discharge at the San Pedro stream gauge, and (d) GRACE-derived monthly terrestrial water storage anomaly equivalent thickness produced by JPL (green) and CSR (blue). Climate intervals are indicated with vertical bars and further detailed in (d) with the timing of large precipitation events.

Figure 4. Freshwater allocation and use in the SdA basin. With (a) allocated freshwater permits divided by water source (symbol shape), use category (symbol color), and allocated amount (symbol size). (b) Pie charts of estimated actual freshwater use in 2014 within each sub-watershed zone divided by use category - lithium mining (black), other mining (grey), agriculture (green), domestic (blue), tourism (purple), and other (orange). No withdrawals occur within the Peine sub-watershed zone. Pie charts in (c) and (d) represent total allocated freshwater permits and estimated actual freshwater use in 2014, respectively.

Figure 5. Annual freshwater and brine withdrawals associated with mining operations in the SdA basin. Minera Escondida Limitada extractions from ended in 2020. The blue bar represents the time frame (2014) of the water use assessment presented in **Figure 4**d.

Figure 6. Distribution of modern/premodern (relic) water content. Pie charts show this ratio grouped by inflow zone (black outline) which includes springs, streams, and groundwaters, and basin floor water bodies (yellow outline). The high elevation lakes Miscanti & Miñiques outside the topographic watershed are included. Black lines delineate zones of flux into the basin and the

approximate outline of the basin floor (as defined by Munk et al., 2018). Light grey lines are 250-meter contours of elevation. Colored dots show all samples collected for this work classified by water type (n=106). (a) Inset cross-sectional schematic defining the physical water body classifications.

Figure 7. Processes controlling physical water distinctions and interactions. Circles are proportional to chloride concentration in each sample. The grey vertical bar is the Global Meteoric Water Line (GMWL), and the blue box represents the approximate range of meteoric input waters (based on Moran et al., 2019 data). Arrows depict the influence of important hydrological processes and interactions. (a) Violin plot of all data grouped by physical water type. Grey boxes show the interquartile range; white dots are the median and the colored polygons represent the frequency distribution of the data (black dots).

Figure 8. Modeled versus observed percent modern values at major sample sites with the line of direct 1:1 relationship. Modeled values are based on the piston flow transit model described in section 4.2. Blue dots are modeled values (K = 10 m/d), high-low range represented by K=15.5 m/d and K= 5 m/d respectively.

Figure 9. Current (DGA) and revised conceptualizations of the SdA basin water budget. Sources of water are on the left side of the Sankey diagrams and sinks are on the right. All terms represent water or brine flux in units of L/s. Precipitation (P) becomes infiltration losses due to evaporation (E_i) or the modern recharge component to surface water (SW) and groundwater (GW). (a) Current DGA conceptualization of the water budget without anthropogenic withdrawals with all SW and GW flux resulting in evaporation on or near the salar floor (E_s). (b) Current DGA conceptualization of the water budget with anthropogenic water withdrawals (W_f) and brine withdrawals (W_b) from storage in the brine body (S_b). (c) Revised conceptualization of the water budget with additional groundwater flux from storage (S). (d) Revised conceptualization of the water budget including anthropogenic withdrawals.

References

AghaKouchak, A., Mirchi, A., Madani, K., Di Baldassarre, G., Nazemi, A., Alborzi, A., … Wanders, N. (2021). Anthropogenic Drought: Definition, Challenges, and Opportunities. Reviews of Geophysics, 59(2), 1–23. https://doi.org/10.1029/2019RG000683

Ahamed, A., Knight, R., Alam, S., Pauloo, R., & Melton, F. (2021). Assessing the utility of remote sensing data to accurately estimate changes in groundwater storage. Science of The Total Environment, 807, 150635. https://doi.org/10.1016/j.scitotenv.2021.150635

AMPHOS21 (2018). Estudio de modelos hidrogeológicos conceptuales integrados, para los salares de Atacama, Maricunga y Pedernales. Comité de Minería No Metálica CORFO, 368.

Ambrose, H., & Kendall, A. (2020). Understanding the future of lithium: Part 1, resource model. Journal of Industrial Ecology, 24(1), 80–89. https://doi.org/10.1111/jiec.12949

Anderson, M., Low, R., & Foot, S. (2002). Sustainable groundwater development in arid, high Andean basins. Geological Society, London, Special Publications, 193(1), 133–144. https://doi.org/10.1144/GSL.SP.2002.193.01.11

Ashraf, S., Nazemi, A., & AghaKouchak, A. (2021). Anthropogenic drought dominates groundwater depletion in Iran. Scientific Reports, 11(1), 9135. https://doi.org/10.1038/s41598-021-88522-y

Babidge, S., Kalazich, F., Prieto, M., & Yager, K. (2019). "That's the problem with that lake; it changes sides": mapping extraction and ecological exhaustion in the Atacama. Journal of Political Ecology, 26(1), 738–760. https://doi.org/10.2458/v26i1.23169

Bambach, N. E., Rhoades, A. M., Hatchett, B. J., Jones, A. D., Ullrich, P. A., & Zarzycki, C. M. (2021). Projecting climate change in South America using variable-resolution Community Earth System Model: An application to Chile. International Journal of Climatology, (August), 1–29. https://doi.org/10.1002/joc.7379

Beria, H., Larsen, J. R., Ceperley, N. C., Michelon, A., Vennemann, T., & Schaefli, B. (2018). Understanding snow hydrological processes through the lens of stable water isotopes. Wiley Interdisciplinary Reviews: Water, (June), e1311. https://doi.org/10.1002/wat2.1311

Bierkens, M. F. P., & Wada, Y. (2019). Non-renewable groundwater use and groundwater depletion: a review. Environmental Research Letters, 14(6), 063002. https://doi.org/10.1088/1748-9326/ab1a5f

Birkel, C., & Soulsby, C. (2015). Advancing tracer-aided rainfall-runoff modelling: a review of progress, problems and unrealised potential. Hydrological Processes, 29(25), 5227–5240. https://doi.org/10.1002/hyp.10594

Blard, P.-H., Sylvestre, F., Tripati, A. K., Claude, C., Causse, C., Coudrain, A., … Lavé, J. (2011). Lake highstands on the Altiplano (Tropical Andes) contemporaneous with Heinrich 1 and the Younger Dryas: new insights from 14C, U–Th dating and δ18O of

carbonates. Quaternary Science Reviews, 30(27–28), 3973–3989. https://doi.org/10.1016/j.quascirev.2011.11.001

Bobst, A. L., Lowenstein, T. K., Jordan, T. E., Godfrey, L. V, Ku, T. L., & Luo, S. (2001). A 106 ka paleoclimate record from drill core of the Salar de Atacama, northern Chile. Palaeogeography, Palaeoclimatology, Palaeoecology, 173(1–2), 21–42. https://doi.org/10.1016/S0031-0182(01)00308-X

Boulay, A.-M., Bare, J., Benini, L., Berger, M., Lathuillière, M. J., Manzardo, A., … Pfister, S. (2018). The WULCA consensus characterization model for water scarcity footprints: assessing impacts of water consumption based on available water remaining (AWARE). The International Journal of Life Cycle Assessment, 23(2), 368–378. https://doi.org/10.1007/s11367-017-1333-8

Boutt, D. F., Hynek, S. A., Munk, L. A., & Corenthal, L. G. (2016). Rapid recharge of fresh water to the halite-hosted brine aquifer of Salar de Atacama, Chile. Hydrological Processes, 30(25), 4720–4740. https://doi.org/10.1002/hyp.10994

Boutt, D.F., Corenthal, L.G., Moran, B.J. et al. Imbalance in the modern hydrologic budget of topographic catchments along the western slope of the Andes (21–25°S): implications for groundwater recharge assessment. Hydrogeol J 29, 985–1007 (2021). https://doi.org/10.1007/s10040-021-02309-z

Bredehoeft, J. D. (2002). The water budget myth revisited: Why hydrogeologists model. Ground Water, Vol. 40, pp. 340–345. https://doi.org/10.1111/j.1745-6584.2002.tb02511.x

Buttle, J.M. (1994). lsotope hydrograph separations and rapid delivery of pre-event water from basins drainage. Phys. Geogr. 18, 16–41.

Cabello, J. (2021). Lithium brine production, reserves, resources and exploration in Chile: An updated review. Ore Geology Reviews, 128(2020), 103883. https://doi.org/10.1016/j.oregeorev.2020.103883

Cartwright, I., Cendón, D., Currell, M., & Meredith, K. (2017). A review of radioactive isotopes and other residence time tracers in understanding groundwater recharge: Possibilities, challenges, and limitations. Journal of Hydrology, 555, 797–811. https://doi.org/10.1016/j.jhydrol.2017.10.053

Clark, I. & Fritz, P. (1997). Environmental Isotopes in Hydrogeology. Lewis Publications, Boca Raton, FL.

Cook, P.G. and Bohlke, J.K. (2000). Determining timescales for groundwater flow and solute transport. In: Cook, P.G., Herczeg, A.L. (Eds.), Environmental Tracers in Subsurface Hydrology. Kluwer, Boston, pp. 1–30.

Cordero, R. R., Asencio, V., Feron, S., Damiani, A., Llanillo, P. J., Sepulveda, E., … Casassa, G. (2019). Dry-Season Snow Cover Losses in the Andes (18°–40°S) driven by Changes in Large-Scale Climate Modes. Scientific Reports, 9(1), 16945. https://doi.org/10.1038/s41598-019-53486-7

Corenthal, L. G., Boutt, D. F., Hynek, S. A., & Munk, L. A. (2016). Regional groundwater flow and accumulation of a massive evaporite deposit at the margin of the Chilean Altiplano.

Geophysical Research Letters, 43(15), 8017–8025. https://doi.org/10.1002/2016GL070076

Cortecci, G., Boschetti, T., Mussi, M., Lameli, C. H., Mucchino, C., & Barbieri, M. (2005). New chemical and original isotopic data on waters from El Tatio geothermal field, northern Chile. Geochemical Journal, 39(6), 547–571. https://doi.org/10.2343/geochemj.39.547

DGA (Dirección General de Aguas) (2013). Análisis de la Oferta Hídrica del Salar de Atacama. Santiago, Chile.

Fan, Y., Li, H., & Miguez-Macho, G. (2013). Global Patterns of Groundwater Table Depth. Science, 339(6122), 940–943. https://doi.org/10.1126/science.1229881

Ferrero, M. E., & Villalba, R. (2019). Interannual and Long-Term Precipitation Variability Along the Subtropical Mountains and Adjacent Chaco (22–29° S) in Argentina. Frontiers in Earth Science, 7(July). https://doi.org/10.3389/feart.2019.00148

Frau, D., Moran, B. J., Arengo, F., Marconi, P., Battauz, Y., Mora, C., … Boutt, D. F. (2021). Hydroclimatological Patterns and Limnological Characteristics of Unique Wetland Systems on the Argentine High Andean Plateau. Hydrology, 8(4), 164. https://doi.org/10.3390/hydrology8040164

Gajardo, G., & Redón, S. (2019). Andean hypersaline lakes in the Atacama Desert, northern Chile: Between lithium exploitation and unique biodiversity conservation. Conservation Science and Practice, 1(9), 1–8. https://doi.org/10.1111/csp2.94

Garreaud, R., Vuille, M., & Clement, A. C. (2003). The climate of the Altiplano: Observed current conditions and mechanisms of past changes. Palaeogeography, Palaeoclimatology, Palaeoecology, 194(1–3), 5–22. https://doi.org/10.1016/S0031-0182(03)00269-4

Garreaud, R. D., Boisier, J. P., Rondanelli, R., Montecinos, A., Sepúlveda, H. H., & Veloso-Aguila, D. (2020). The Central Chile Mega Drought (2010–2018): A climate dynamics perspective. International Journal of Climatology, 40(1), 421–439. https://doi.org/10.1002/joc.6219

Garreaud, R. D., Clem, K., & Veloso, J. V. (2021). The South Pacific Pressure Trend Dipole and the Southern Blob. Journal of Climate, 34(18), 7661–7676. https://doi.org/10.1175/JCLI-D-20-0886.1

Gayo, E. M., Latorre, C., Jordan, T. E., Nester, P. L., Estay, S. A., Ojeda, K. F., & Santoro, C. M. (2012). Late Quaternary hydrological and ecological changes in the hyperarid core of the northern Atacama Desert (~21°S). Earth-Science Reviews, 113(3–4), 120–140. https://doi.org/10.1016/j.earscirev.2012.04.003

Gleeson, T., Marklund, L., Smith, L., & Manning, A. H. (2011). Classifying the water table at regional to continental scales. Geophysical Research Letters, 38(5), n/a-n/a. https://doi.org/10.1029/2010GL046427

Godfrey, L.., Jordan, T.., Lowenstein, T.., & Alonso, R. (2003). Stable isotope constraints on the transport of water to the Andes between 22° and 26°S during the last glacial cycle.

Palaeogeography, Palaeoclimatology, Palaeoecology, 194(1–3), 299–317. https://doi.org/10.1016/S0031-0182(03)00283-9

Grosjean, Martin; Geyh, Mebus A.; Messerli, Bruno; Schotterer, U. (1995). Late-glacial and early Holocene lake sediments, groundwater formation and climate in the Atacama Altiplano 22-24°S. Journal of Paleolimnology, 14, 241–252.

Grosjean, M., & Núñez, A. L. (1994). Lateglacial, early and middle holocene environments, human occupation, and resource use in the Atacama (Northern Chile). Geoarchaeology, 9(4), 271–286. https://doi.org/10.1002/gea.3340090402

Gutiérrez, J. S., Navedo, J. G., & Soriano-Redondo, A. (2018). Chilean Atacama site imperilled by lithium mining. Nature, 557(7706), 492–492. https://doi.org/10.1038/d41586-018-05233-7

Herrera, C., Custodio, E., Chong, G., Lambán, L. J., Riquelme, R., Wilke, H., … Lictevout, E. (2016). Groundwater flow in a closed basin with a saline shallow lake in a volcanic area: Laguna Tuyajto, northern Chilean Altiplano of the Andes. Science of The Total Environment, 541, 303–318. https://doi.org/10.1016/j.scitotenv.2015.09.060

Houston, J. (2002). Groundwater recharge through an alluvial fan in the Atacama Desert, northern Chile: mechanisms, magnitudes and causes. Hydrological Processes, 16(15), 3019–3035. https://doi.org/10.1002/hyp.1086

Houston, J. (2006). Variability of precipitation in the Atacama Desert: Its causes and hydrological impact. International Journal of Climatology, 26(July), 2181–2198. https://doi.org/10.1002/joc

Houston, J. (2007). Recharge to groundwater in the Turi Basin, northern Chile: An evaluation based on tritium and chloride mass balance techniques. Journal of Hydrology, 334(3–4), 534–544. https://doi.org/10.1016/j.jhydrol.2006.10.030

Houston, J. (2009). A recharge model for high altitude, arid, Andean aquifers. Hydrological Processes, 23(16), 2383–2393. https://doi.org/10.1002/hyp.7350

Houston, J., & Hart, D. (2004). Theoretical head decay in closed basin aquifers: an insight into fossil groundwater and recharge events in the Andes of northern Chile. Quarterly Journal of Engineering Geology and Hydrogeology, 37(2), 131–139. https://doi.org/10.1144/1470-9236/04-007

Jasechko, S. (2016). Partitioning young and old groundwater with geochemical tracers. Chemical Geology, 427, 35–42. https://doi.org/10.1016/j.chemgeo.2016.02.012

Jones, D. B., Harrison, S., Anderson, K., & Whalley, W. B. (2019). Rock glaciers and mountain hydrology: A review. Earth-Science Reviews, 193, 66–90. https://doi.org/10.1016/j.earscirev.2019.04.001

Jordan, T. E., Munoz, N., Hein, M., Lowenstein, T., Godfrey, L., & Yu, J. (2002). Active faulting and folding without topographic expression in an evaporite basin, Chile. Bulletin of the Geological Society of America, 114(11), 1406–1421. https://doi.org/10.1130/0016-7606(2002)114<1406:AFAFWT>2.0.CO;2

Jordan, T. E., Herrera L., C., Godfrey, L. V., Colucci, S. J., Gamboa P., C., Urrutia M., J., … Paul, J. F. (2019). Isotopic characteristics and paleoclimate implications of the extreme precipitation event of March 2015 in northern Chile. Andean Geology, 46(1), 1. https://doi.org/10.5027/andgeoV46n1-3087

Kendall, C. & Caldwell. E.A. (1998) Fundamentals of isotope geochemistry. In: Isotope Tracers in Catchment Hydrology (Eds C. Kendall & J.J. McDonnell), pp. 51-86. Elsevier, Amsterdam.

Kendall, C., McDonnell, J.J. (1998). Isotope Tracers in Catchment Hydrology. 839 pp. Elsevier, New York

Kesler, S. E., Gruber, P. W., Medina, P. A., Keoleian, G. A., Everson, M. P., & Wallington, T. J. (2012). Global lithium resources: Relative importance of pegmatite, brine and other deposits. Ore Geology Reviews, 48, 55–69. https://doi.org/10.1016/j.oregeorev.2012.05.006

Kinnard, C., Ginot, P., Surazakov, A., MacDonell, S., Nicholson, L., Patris, N., … Squeo, F. A. (2020). Mass Balance and Climate History of a High-Altitude Glacier, Desert Andes of Chile. Frontiers in Earth Science, 8(February), 1–20. https://doi.org/10.3389/feart.2020.00040

Landerer, F. 2021. TELLUS_GRAC_L3_CSR_RL06_LND_v04. Ver. RL06 v04. PO.DAAC, CA, USA. Dataset accessed [2021-02-14] at https://doi.org/10.5067/TELND-3AC64.Oyarzún, J., & Oyarzún, R. (2011). Sustainable development threats, inter-sector conflicts and environmental policy requirements in the arid, mining rich, northern Chile territory. Sustainable Development, 19(4), 263–274. https://doi.org/10.1002/sd.441

Landerer, F. W., & Swenson, S. C. (2012). Accuracy of scaled GRACE terrestrial water storage estimates. Water Resources Research, 48(4), 1–11. https://doi.org/10.1029/2011WR011453

Langenbrunner, B., Pritchard, M. S., Kooperman, G. J., & Randerson, J. T. (2019). Why Does Amazon Precipitation Decrease When Tropical Forests Respond to Increasing CO^2. Earth's Future, 7(4), 450–468. https://doi.org/10.1029/2018EF001026

Liu, W., Agusdinata, D. B., & Myint, S. W. (2019). Spatiotemporal patterns of lithium mining and environmental degradation in the Atacama Salt Flat, Chile. International Journal of Applied Earth Observation and Geoinformation, 80(January), 145–156. https://doi.org/10.1016/j.jag.2019.04.016

Liu, W., & Agusdinata, D. B. (2020). Interdependencies of lithium mining and communities sustainability in Salar de Atacama, Chile. Journal of Cleaner Production, 260, 120838. https://doi.org/10.1016/j.jclepro.2020.120838

Liu, Y., Wagener, T., Beck, H. E., & Hartmann, A. (2020). What is the hydrologically effective area of a catchment? Environmental Research Letters, 15(10), 104024. https://doi.org/10.1088/1748-9326/aba7e5

Masbruch, M. D., Rumsey, C. A., Gangopadhyay, S., Susong, D. D., & Pruitt, T. (2016). Analyses of infrequent (quasi-decadal) large groundwater recharge events in the northern

Great Basin: Their importance for groundwater availability, use, and management. Water Resources Research, 52(10), 7819–7836. https://doi.org/10.1002/2016WR019060

MEL (Minera Escondida Ltda) (2017). Informe “Plan de Alerta Temprana para el Acuífero Monturaqui-Negrillar-Tilopozo”. Santiago, Chile

McDonnell, J. J. (2017). Beyond the water balance. Nature Geoscience, 10(6), 396–396. https://doi.org/10.1038/ngeo2964

McKnight, S. V., Boutt, D. F., & Munk, L. A. (2021). Impact of Hydrostratigraphic Continuity on Brine-to-Freshwater Interface Dynamics: Implications From a Two-Dimensional Parametric Study in an Arid and Endorheic Basin. Water Resources Research, 57(4). https://doi.org/10.1029/2020WR028302

Montecino, H. C., Staub, G., Ferreira, V. G., & Parra, L. B. (2016). MONITORING GROUNDWATER STORAGE IN NORTHERN CHILE BASED ON SATELLITE OBSERVATIONS AND DATA SIMULATION. Boletim de Ciências Geodésicas, 22(1), 1–15. https://doi.org/10.1590/S1982-21702016000100001

Morales, M. S., Cook, E. R., Barichivich, J., Christie, D. A., Villalba, R., LeQuesne, C., … Boninsegna, J. A. (2020). Six hundred years of South American tree rings reveal an increase in severe hydroclimatic events since mid-20th century. Proceedings of the National Academy of Sciences, 117(29), 16816–16823. https://doi.org/10.1073/pnas.2002411117

Moran, B. J., Boutt, D. F., & Munk, L. A. (2019). Stable and Radioisotope Systematics Reveal Fossil Water as Fundamental Characteristic of Arid Orogenic-Scale Groundwater Systems. Water Resources Research, 55(12), 11295–11315. https://doi.org/10.1029/2019WR026386

Moran, Brendan J.; Boutt, David F.; McKnight, Sarah V.; Jenckes, Jordan; Munk, Lee Ann; Corkran, Daniel; and Kirshen, Alexander, "Data for "Relic Groundwater and Mega Drought Confound Interpretations of Water Sustainability and Lithium Extraction in Arid Lands"" (2021). Data and Datasets. 145. https://scholarworks.umass.edu/data/145

Moran, Brendan J., "Fundamental Controls on the Water Cycle in Arid Environments: a Mechanistic Framework for Spatiotemporal Connectivity Between Hydroclimate and Groundwaters in the Dry Andes" (2022). Doctoral Dissertations. https://scholarworks.umass.edu/dissertations_2/1

Munk, L.A., Hynek, S.A., Bradley, D.C., Boutt, D.F., Labay, K., Jochens, H., (2016). Lithium Brines: A Global Perspective, in Verplanck, P.L. and Hitzman, M.W., eds., Rare Earth and Critical Elements in Ore Deposits. Reviews in Economic Geology (18), 339–365.

Munk, L. A., Boutt, D. F., Hynek, S. A., & Moran, B. J. (2018). Hydrogeochemical fluxes and processes contributing to the formation of lithium-enriched brines in a hyper-arid continental basin. Chemical Geology, 493, 37–57. https://doi.org/10.1016/j.chemgeo.2018.05.013

Munk, L. A., Boutt, D. F., Moran, B. J., McKnight, S. V., & Jenckes, J. (2021). Hydrogeologic and geochemical distinctions in freshwater-brine systems of an Andean salar.

Geochemistry, Geophysics, Geosystems, 22, e2020GC009345. https://doi.org/10.1029/2020GC009345

Pabón-Caicedo, J. D., Arias, P. A., Carril, A. F., Espinoza, J. C., Borrel, L. F., Goubanova, K., … Villalba, R. (2020). Observed and Projected Hydroclimate Changes in the Andes. Frontiers in Earth Science, 8(March), 1–29. https://doi.org/10.3389/feart.2020.00061

Pascale, S., Carvalho, L. M. V, Adams, D. K., Castro, C. L., & Cavalcanti, I. F. A. (2019). Current and Future Variations of the Monsoons of the Americas in a Warming Climate. Current Climate Change Reports. https://doi.org/10.1007/s40641-019-00135-w

Pekel, J.-F., Cottam, A., Gorelick, N., & Belward, A. S. (2016). High-resolution mapping of global surface water and its long-term changes. Nature, 540(7633), 418–422. https://doi.org/10.1038/nature20584

Pfeiffer, M., Latorre, C., Santoro, C. M., Gayo, E. M., Rojas, R., Carrevedo, M. L., … Amundson, R. (2018). Chronology, stratigraphy and hydrological modelling of extensive wetlands and paleolakes in the hyperarid core of the Atacama Desert during the late quaternary. Quaternary Science Reviews, 197, 224–245. https://doi.org/10.1016/j.quascirev.2018.08.001

Pfister, S., Koehler, A., & Hellweg, S. (2009). Assessing the Environmental Impacts of Freshwater Consumption in LCA. Environmental Science & Technology, 43(11), 4098–4104. https://doi.org/10.1021/es802423e

Placzek, C. J., Quade, J., & Patchett, P. J. (2013). A 130ka reconstruction of rainfall on the Bolivian Altiplano. Earth and Planetary Science Letters, 363, 97–108. https://doi.org/10.1016/j.epsl.2012.12.017

Quade, J., Rech, J. a., Betancourt, J. L., Latorre, C., Quade, B., Rylander, K. A., & Fisher, T. (2008). Paleowetlands and regional climate change in the central Atacama Desert, northern chile. Quaternary Research, 69(03), 343–360. https://doi.org/10.1016/j.yqres.2008.01.003

Reager, J. T., & Famiglietti, J. S. (2013). Characteristic mega-basin water storage behavior using GRACE. Water Resources Research, 49(6), 3314–3329. https://doi.org/10.1002/wrcr.20264

Rech, J. a., Pigati, J. S., Quade, J., & Betancourt, J. L. (2003). Re-evaluation of mid-Holocene deposits at Quebrada Puripica, northern Chile. Palaeogeography, Palaeoclimatology, Palaeoecology, 194(1–3), 207–222. https://doi.org/10.1016/S0031-0182(03)00278-5

Ridoutt, B. G., & Pfister, S. (2010). A revised approach to water footprinting to make transparent the impacts of consumption and production on global freshwater scarcity. Global Environmental Change, 20(1), 113–120. https://doi.org/10.1016/j.gloenvcha.2009.08.003

Rissmann, C., Leybourne, M., Benn, C., & Christenson, B. (2015). The origin of solutes within the groundwaters of a high Andean aquifer. Chemical Geology, 396, 164–181. https://doi.org/10.1016/j.chemgeo.2014.11.029

1178 Rivera, J. A., Otta, S., Lauro, C., & Zazulie, N. (2021). A Decade of Hydrological Drought in
1179 Central-Western Argentina. Frontiers in Water, 3(April), 1–20.
1180 https://doi.org/10.3389/frwa.2021.640544

1181 Rooyen, J. D., Watson, A. P., Palcsu, L., & Miller, J. A. (2021). Constraining the Spatial
1182 Distribution of Tritium in Groundwater Across South Africa. Water Resources Research,
1183 57(8). https://doi.org/10.1029/2020WR028985

1184 Scanlon, B. R., Keese, K. E., Flint, A. L., Flint, L. E., Gaye, C. B., Edmunds, W. M., &
1185 Simmers, I. (2006). Global synthesis of groundwater recharge in semiarid and arid
1186 regions. Hydrological Processes, 20(15), 3335–3370. https://doi.org/10.1002/hyp.6335

1187 Schaffer, N., MacDonell, S., Réveillet, M., Yáñez, E., & Valois, R. (2019). Rock glaciers as a
1188 water resource in a changing climate in the semiarid Chilean Andes. Regional
1189 Environmental Change, 19(5), 1263–1279. https://doi.org/10.1007/s10113-018-01459-3

1190 Schaller, M. F., & Fan, Y. (2009). River basins as groundwater exporters and importers:
1191 Implications for water cycle and climate modeling. Journal of Geophysical Research,
1192 114(D4), D04103. https://doi.org/10.1029/2008JD010636

1193 Schomberg, A. C., Bringezu, S., & Flörke, M. (2021). Extended life cycle assessment reveals the
1194 spatially-explicit water scarcity footprint of a lithium-ion battery storage.
1195 Communications Earth & Environment, 2(1), 11. https://doi.org/10.1038/s43247-020-
1196 00080-9

1197 Somers, L. D., & McKenzie, J. M. (2020). A review of groundwater in high mountain
1198 environments. WIREs Water, 7(6). https://doi.org/10.1002/wat2.1475

1199 Sonter, L. J., Dade, M. C., Watson, J. E. M., & Valenta, R. K. (2020). Renewable energy
1200 production will exacerbate mining threats to biodiversity. Nature Communications, 11(1),
1201 4174. https://doi.org/10.1038/s41467-020-17928-5

1202 Steiger, N. J., Smerdon, J. E., Seager, R., Williams, A. P., & Varuolo-Clarke, A. M. (2021).
1203 ENSO-driven coupled megadroughts in North and South America over the last
1204 millennium. Nature Geoscience, 14(10), 739–744. https://doi.org/10.1038/s41561-021-
1205 00819-9

1206 Stewart, M. K., Morgenstern, U., Gusyev, M. A., & Maloszewski, P. (2017). Aggregation effects
1207 on tritium-based mean transit times and young water fractions in spatially heterogeneous
1208 catchments and groundwater systems, and implications for past and future applications of
1209 tritium. Hydrology and Earth System Sciences Discussions, (October), 1–26.
1210 https://doi.org/10.5194/hess-2016-532

1211 Stonestrom, D., & Harrill, R. (2007). Ground-Water Recharge in the Arid and Semiarid
1212 Southwestern United States—Climatic and Geologic Framework. Ground-Water
1213 Resources Program; National Research Program, (1703), Chapter A. Retrieved from
1214 http://pubs.er.usgs.gov/thumbnails/usgs_thumb.jpg%5Cnhttp://pubs.usgs.gov/pp/pp1703/

1215 Valdivielso, S., Vázquez-Suñé, E., & Custodio, E. (2020). Origin and variability of oxygen and
1216 hydrogen isotopic composition of precipitation in the Central Andes: A review. Journal

of Hydrology, 587(December 2019), 124899. https://doi.org/10.1016/j.jhydrol.2020.124899

Vuille, M., & Ammann, C. (1997). Regional snowfall patterns in the high, arid Andes. Climatic Change, 36, 413–423. https://doi.org/10.1007/978-94-015-8905-5_10

Wada, Y., Bierkens, M. F. P., de Roo, A., Dirmeyer, P. A., Famiglietti, J. S., Hanasaki, N., … Wheater, H. (2017). Human–water interface in hydrological modelling: current status and future directions. Hydrology and Earth System Sciences, 21(8), 4169–4193. https://doi.org/10.5194/hess-21-4169-2017

Wang, J., Song, C., Reager, J. T., Yao, F., Famiglietti, J. S., Sheng, Y., … Wada, Y. (2018). Recent global decline in endorheic basin water storages. Nature Geoscience, 11(12), 926–932. https://doi.org/10.1038/s41561-018-0265-7

Wiese, D. N., Landerer, F. W., & Watkins, M. M. (2016). Quantifying and reducing leakage errors in the JPL RL05M GRACE mascon solution. Water Resources Research, 52(9), 7490–7502. https://doi.org/10.1002/2016WR019344

Zipper, S. C., Jaramillo, F., Wang-Erlandsson, L., Cornell, S. E., Gleeson, T., Porkka, M., … Gordon, L. (2020). Integrating the Water Planetary Boundary With Water Management From Local to Global Scales. Earth's Future, 8(2). https://doi.org/10.1029/2019EF001377

References from Supporting Information

Clarke, W.B., Jenkins, W.J., Top, Z. (1976). Determination of tritium by mass spectrometric measurement of 3He. Int. J. Appl. Radiat. Isot. 27 (9), 515e522.

Condom, T., Martínez, R., Pabón, J. D., Costa, F., Pineda, L., Nieto, J. J., … Villacis, M. (2020). Climatological and Hydrological Observations for the South American Andes: In situ Stations, Satellite, and Reanalysis Data Sets. Frontiers in Earth Science, 8(April), 1–20. https://doi.org/10.3389/feart.2020.00092

Dubey, S., Gupta, H., Goyal, M. K., & Joshi, N. (2021). Evaluation of precipitation datasets available on Google earth engine over India. International Journal of Climatology, 41(10), 4844–4863. https://doi.org/10.1002/joc.7102

Eshel, G., Araus, V., Undurraga, S., Soto, D. C., Moraga, C., Montecinos, A., … Gutiérrez, R. A. (2021). Plant ecological genomics at the limits of life in the Atacama Desert. Proceedings of the National Academy of Sciences, 118(46), e2101177118. https://doi.org/10.1073/pnas.2101177118

Gorelick, N., Hancher, M., Dixon, M., Ilyushchenko, S., Thau, D. and Moore, R. (2017) Google earth engine: planetary-scale geospatial analysis for everyone. Remote Sensing of Environ- ment, 202, 18–27. https://doi.org/10.1016/j.rse.2017.06.031.

Hipel, K.W. and McLeod, A.I. (1994), Time Series Modelling of Water Resources and Environmental Systems. New York: Elsevier Science.

Hirsch, R. M., Slack, J. R., and Smith, R. A. (1982), Techniques of trend analysis for monthly water quality data, Water Resour. Res., 18(1), 107– 121, doi:10.1029/WR018i001p00107.

Hussain et al., (2019). pyMannKendall: a python package for non parametric Mann Kendall family of trend tests. Journal of Open Source Software, 4(39), 1556, https://doi.org/10.21105/joss.01556

Jordan, T. E., Mpodozis, C., Muñoz, N., Blanco, N., Pananont, P., & Gardeweg, M. (2007). Cenozoic subsurface stratigraphy and structure of the Salar de Atacama Basin, northern Chile. Journal of South American Earth Sciences, 23(2–3), 122–146. https://doi.org/10.1016/j.jsames.2006.09.024

Lucas, L., & Unterweger, M. (2000). Comprehensive review and critical evaluation of the half-life of tritium. Journal of Research of the National Institute of Standards and Technology, 105(4), 541–549. https://doi. org/10.6028/jres.105.043

MEL (Minera Escondida Ltda) (2017). Informe "Plan de Alerta Temprana para el Acuífero Monturaqui-Negrillar-Tilopozo". Santiago, Chile

NASA. (2000). Measuring Vegetation, Normalized Difference Vegetation Index (NDVI) https://www.usgs.gov/core-science-systems/eros/phenology/science/ndvi-foundation-remote-sensing-phenology?qt-science_center_objects=0#qt-science_center_objects.

Rubilar, J., Martínez, F., Arriagada, C., Becerra, J., & Bascuñán, S. (2018). Structure of the Cordillera de la Sal: A key tectonic element for the Oligocene-Neogene evolution of the Salar de Atacama basin, Central Andes, northern Chile. Journal of South American Earth Sciences, 87, 200–210. https://doi.org/10.1016/j.jsames.2017.11.013

Salio, P., Hobouchian, M. P., García Skabar, Y., & Vila, D. (2015). Evaluation of high-resolution satellite precipitation estimates over southern South America using a dense rain gauge network. Atmospheric Research, 163, 146–161. https://doi.org/10.1016/j.atmosres.2014.11.017

Schween, J. H., Hoffmeister, D., & Löhnert, U. (2020). Filling the observational gap in the Atacama Desert with a new network of climate stations. Global and Planetary Change, 184(May 2019), 103034. https://doi.org/10.1016/j.gloplacha.2019.103034

Tucker C.J. (1979) Red and photographic infrared linear combinations monitoring vegetation. Journal of Remote Sensing Environment, 8(2), 127-150. doi:10.1016/0034-4257(79)90013-0

USGS (U.S. Geological Survey) (2018). NDVI, the Foundation for Remote Sensing Phenology. https://www.usgs.gov/core-science-systems/eros/phenology/science/ndvi-foundation-remote-sensing-phenology?qt-science_center_objects=0#qt-science_center_objects

USGS (U.S. Geological Survey) (2022). Mineral commodity summaries 2022: U.S. Geological Survey, 202 p., https://doi.org/10.3133/mcs2022.

Earth's Future

Supporting Information for:

Water Sustainability, Drought, Relic Groundwater and Lithium Resource Extraction in an Arid Landscape

B. J. Moran[1] 0000-0002-9862-6241, D. F. Boutt[1] 0000-0003-1397-0279, S. V. McKnight[1] 0000-0002-6013-193X, J. Jenckes[2] 0000-0002-1811-3076, L. A. Munk[2] 0000-0003-2850-545X, Daniel Corkan[1] 0000-0001-6168-8281, Alexander Kirshen[1] 0000-0003-2015-4085

[1]Department of Geosciences, University of Massachusetts Amherst

[2]Department of Geological Sciences, University of Alaska Anchorage

Corresponding author: Brendan Moran, bmoran@geo.umass

Contents of this file

Introduction

The supporting information contained in this section includes additional details on the methodologies used in this work including analytical methods description, assessment of remotely sensed data, and detailed descriptions of water budget calculations and groundwater level changes.

Text S1. Expanded Methods

Expanded Remotely Sensed Data Collection Methods

The JRC imagery dataset is constructed using Landsat imagery compiled from 1984 through 2020; we accessed and extracted these data using Google Earth Engine (GEE) (Gorelick et al., 2017). The JRC imagery defines each pixel as either containing water or not containing water. We defined a polygon that encompassed the Region of Interest (ROI); these ROIs were then used to clip the JRC dataset. To create a time series of monthly water extents we looped through the JRC Monthly Water History and summed the number of pixels within the ROI that were categorized as water. The pixels were then summed into a geographic area using a set of off-the-shelf functions provided by the GEE API.

To assess changes in vegetation cover we utilized the Normalized Difference Vegetation Index (NDVI) which is calculated from spectral imagery using the formula:

$$NDVI = \frac{NIR - RED}{NIR + RED}$$

where NIR is the reflection in the near-infrared spectrum and RED is the reflection in the red range of the spectrum (Tucker, 1979). NDVI is designed to assess the density of vegetation at a given location at a given time. It provides a single band with a range of -1.0 to 1.0 where negative values are clouds, water, and snow; values close to 0 up to 0.1 are rocks and bare soil. Different types of vegetation are classified in values greater than ~0.1. In this case, to be conservative and to be sure we are assessing only living vegetation (not water, soil, or potential errors at the upper boundary of the index) we extracted the pixels whose values were between 0.2 and 0.9 (NASA, 2000; USGS, 2018).

Expanded Remotely Sensed Precipitation Analysis

Through an extensive analysis of available high resolution remotely sensed and gridded precipitation datasets including TRMM-3B43, GPM-IMERG, CHIRPS, ERA5, PERSIANN-CDR, and Cr2Met, we determined that TerraClimate most closely matched both the trends and magnitudes of precipitation observed at terrestrial meteorological

stations in the SdA basin and predicted the most reasonable values of precipitation in ungauged areas based on estimates of elevation-precipitation relationships (e.g. Houston, 2009; Boutt et al., 2021). As noted by Salio et al. (2015), Schween et al. (2020), and Condom et al., (2020), satellite microwave observations such as those utilized by TRMM and GPM tend to overestimate precipitation, particularly in arid areas and over complex topography where these errors can be up to two orders of magnitude. Our analysis of these products showed overestimations at terrestrial stations of generally greater than one order of magnitude. Gridded interpolation products such as CHIRPS and PERSIANN also appear to be overestimating precipitation in the region. Since these products rely on rain gauges for calibration and interpolation of infrared remotely sensed precipitation data and since all the gauges at SdA are below 3,250 m.a.s.l., large areas of this vast basin are ungauged, particularly the high elevations. As a result, it appears the issues with interpolation likely stem from misrepresentations of these ungauged areas. CHIRPS performed somewhat better than PERSIANN at estimating precipitation values at meteorological stations perhaps due to its higher resolution, however, they both consistently overestimated precipitation by a factor of 2-3. Even the Cr2Met gridded dataset produced by the Chilean Center for Climate and Resilience Research appears to systematically overestimate precipitation amounts at ground-based meteorological stations in the basin. Another recent study with data from 2016-2019 at two meteorological stations on the eastern slope of SdA at 3,060 and 4,090 m.a.s.l. recorded average annual precipitation of 122 mm and 150 mm respectively, agreeing quite well with the TerraClimate estimates (Eshel et al., 2021). Though we do observe overestimates and underestimates in the TerraClimate dataset compared to station data, the magnitude is commonly less than other products we assessed and therefore we believe it is the best basin-scale reflection of precipitation for the region available. This is also supported by recent work by Dubey et al. (2021) that outlines the strengths of this dataset.

Expanded Water Sample Analyses Method

Tritium activity in water samples was measured at the Dissolved and Noble Gas Laboratory, University of Utah. Samples were collected in 1 L HDPE bottles with

minimal headspace. In the lab, 0.5 L aliquots were distilled to remove dissolved solids. These water samples were then degassed in stainless steel flasks until <0.01% of dissolved gas remained and sealed to ingrow helium. ^{3}H concentrations were measured by helium ingrowth (Clarke et al., 1976); 6–12 weeks is typically adequate to ingrow sufficient ^{3}He from the decay of ^{3}H ($t^{1/2}$ = 12.32 yr.; Lucas & Unterweger, 2000) for analysis. ^{3}He concentrations were then measured on a MAP215-50 magnetic sector mass spectrometer using an electron multiplier to measure low abundance ^{3}He, which was directly correlated with the amount of ^{3}H decayed. Data are reported in tritium units (TU) on the date of sampling, where one TU is equivalent to one tritium atom per 10^{18} hydrogen atoms ($^{3}H/H*10^{18}$) (Kendall & Caldwell, 1998). Several duplicate analyses of the same sample were conducted to confirm important values, and the reproducibility for these samples is of the same order as the precision of the measurement. The analytical error associated with each sample is reported along with the results in Table S1.

Water samples were analyzed for $\delta^{2}H$ and $\delta^{18}O$ using wave-length scanned cavity ring-down spectroscopy (Picarro L-1102i); samples were vaporized at 120°C (150°C for higher salt content waters) in the Stable Isotope Laboratory at the University of Alaska – Anchorage. International reference standards (IAEA, Vienna, Austria) were used to calibrate the instrument to the VSMOW-VSLAP scale and working standards (USGS45: $\delta^{2}H$ = -10.3‰, $\delta^{18}O$ = -2.24‰ and USGS46: δ2H = -235.8‰, $\delta^{18}O$ = -29.8‰) were used with each analytical run to correct for instrumental drift. Long-term mean and standard deviation records of a purified water laboratory internal QA/QC standard ($\delta^{2}H$ = -149.80‰, $\delta^{18}O$ = -19.68‰) yield an instrumental precision of 0.93‰ for $\delta^{2}H$ and 0.08‰ for $\delta^{18}O$.

Water samples analyzed for chloride compositions were filtered through 0.45 μm filters using a plastic 60 mL syringe and were stored in clean HDPE bottles. They were analyzed using a consistent, standardized procedure across two laboratories. Samples collected between 2011 and 2018 were analyzed at the University of Alaska Anchorage using an ion chromatograph (Dionex ICS 5000+) and those collected in 2021 were analyzed at the University of Massachusetts Amherst using high-pressure ion chromatography (Dionex Integrion HPIC). Waters with relatively high TDS were diluted volumetrically before analysis. Quantification was performed using seven external

calibration standards ranging from 0.1 to 100 ppb. An IonPac AS15 2×250mm column was used for anion separation using 38mM KOH as eluent and ASRS 300 zero reagent suppressor. The sample injection volume was 10 μL and quantification was performed using five external calibration standards ranging from 0 ppm to 10 ppm. Calibration verification standards and blanks were run every 10th analysis for anions. Anion analysis was verified with a secondary anion standard (Anion II Std Dionex). Samples that exceeded the calibration by 120% were diluted and re-analyzed. A charge balance assessment of these data was also done and only samples having less than 10% error were included.

Expanded Water Use Qualification Method

The 'lithium & potash mining' category was determined using SQM and Albemarle freshwater pumping data from 2014, as they are the only lithium companies using freshwater in the basin. We calculated the 'other mining' category using 2014 Minera Escondida Limitada and Compania Minera Zaldivar data. The total allocated freshwater for these two companies based on the DGA database is 2,148.7 L·s-1. Of that allocation, 1,493 L·s-1 was used in 2014, which is a ratio of 0.69. We further differentiate lithium & potash mining from other mining activities given the history of copper mining in the basin. Additional 'other mining' permits comprise 22.8 L·s-1. Because no pumping data is available for these users, the above ratio of 0.69 was applied to these allocations for an estimated actual use of 15.8 L·s-1. The only exceptions to this estimate are four concessions currently owned by the Wealth Minerals company, which are in the northern area of the salar and which, as confirmed through local experts, have never been utilized; thus, we negated the estimated use for those allocations (600 L·s-1). We rely on previous estimations of non-industrial freshwater use reported by DGA because of their relatively undocumented activities. The most recent estimates for actual use of allocated water extraction for domestic, tourism, and agricultural use are 75%, 75%, and 40%, respectively.

Text S2. Water Budget Calculations

We compare water budgets from two primary sources, the water budget currently in use by the DGA to manage water use within the SdA basin (DGA, 2013), and a revised conceptualization of the water budget (Boutt et al., 2021). We then incorporate anthropogenic water use estimates from this study into these water budgets. In the DGA water budget (Figure 9a), Precipitation (P) and Evapotranspiration from the salar (E_s) estimates are derived from DGA calculations (DGA, 2013). Based on stable isotope analyses (Godfrey et al., 2003), surface water flux (SW) and groundwater flux (GW) is estimated to be 1/3 and 2/3 of E_s, respectively. In the revised water budget (Figure 9c), P, P recharge to SW and GW, net storage flux (S), and E_s are from the most current understanding of the water budget for the basin (Boutt et al., 2021). For both the DGA and revised water budgets, the remainder of P that does not become modern recharge is assumed to become infiltration losses due to evaporation (E_i).

In the post-development scenarios for both the DGA (Figure 9b) and revised (Figure 9d) conceptualizations, anthropogenic freshwater withdrawals (W_f) and brine withdrawals (W_b) are applied to the water budget. The W_f flux from SW and GW is the estimated actual freshwater use in 2014, presented in Section 4.2 and Figure 4. We assume that any diversion of SW or GW flux to W_f results in an equal decrease in SW or GW flux to E_s, and the E_s is reduced accordingly for both post-development scenarios. We assume that all W_b flux results in a corresponding net storage flux from the brine body (S_b).

Text S3. Groundwater Storage Changes

We compiled groundwater level measurements from the SQM environmental monitoring database, Comité de Minería No Metálica CORFO (AMPHOS21, 2018), and Minera Escondida Ltda (MEL, 2017) to establish a record of groundwater level measurements from 94 monitoring points collected between September 1986 and March 2021. For each of the monitoring points, we performed a seasonal Mann-Kendall trend analysis (Hirsch et al., 1982) using pyMannKendall (Hussain et al., 2019) to assess groundwater levels from December 2007 through December 2016. This represents the longest period of continuous groundwater level records for the 94 monitoring points. We used the seasonal Sen's slope (Hipel & McLeod 1994) for the seasonal Mann-Kendall

trend to estimate the mean change in groundwater elevation for the period from December 2007 through December 2016 at each well. We then grouped the wells by the major SdA basin watershed zones (Munk et al., 2018), specified as Diffuse North East gw (n=7), Diffuse North Tumisa gw (n=16), Diffuse South Tumisa gw (n=3), Peine (n=1), and Monturaqui/Negrillar/Tilopozo (MNT) (n=8). In addition, wells located in the salar nucleus were grouped into the West Nucleus (n=24) and East Nucleus (n=35), separated by approximate location of the salar fault system (Jordan et al., 2007, Rubilar et al., 2018). We then calculated the geometric mean of the hydraulic head changes within each zone to estimate the mean for the whole watershed or nucleus zone. Using the mean change in hydraulic head estimates, we calculated the change in groundwater storage for each watershed or nucleus zone assuming a specific yield of 0.25 and using the geodesic area of the zone.

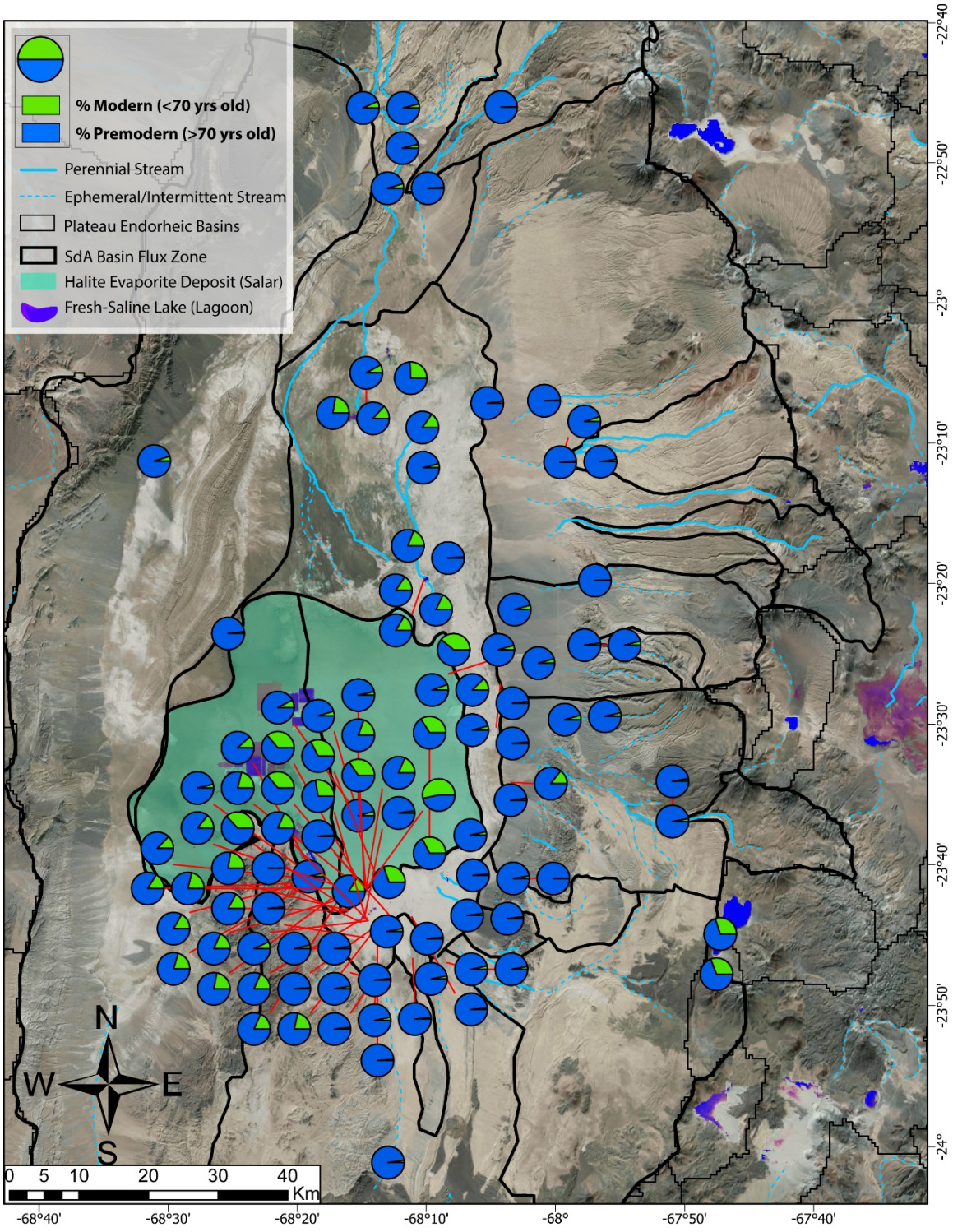

Figure S1. The percent modern water content of all samples presented in this work (n=106). Each circle represents one sample.

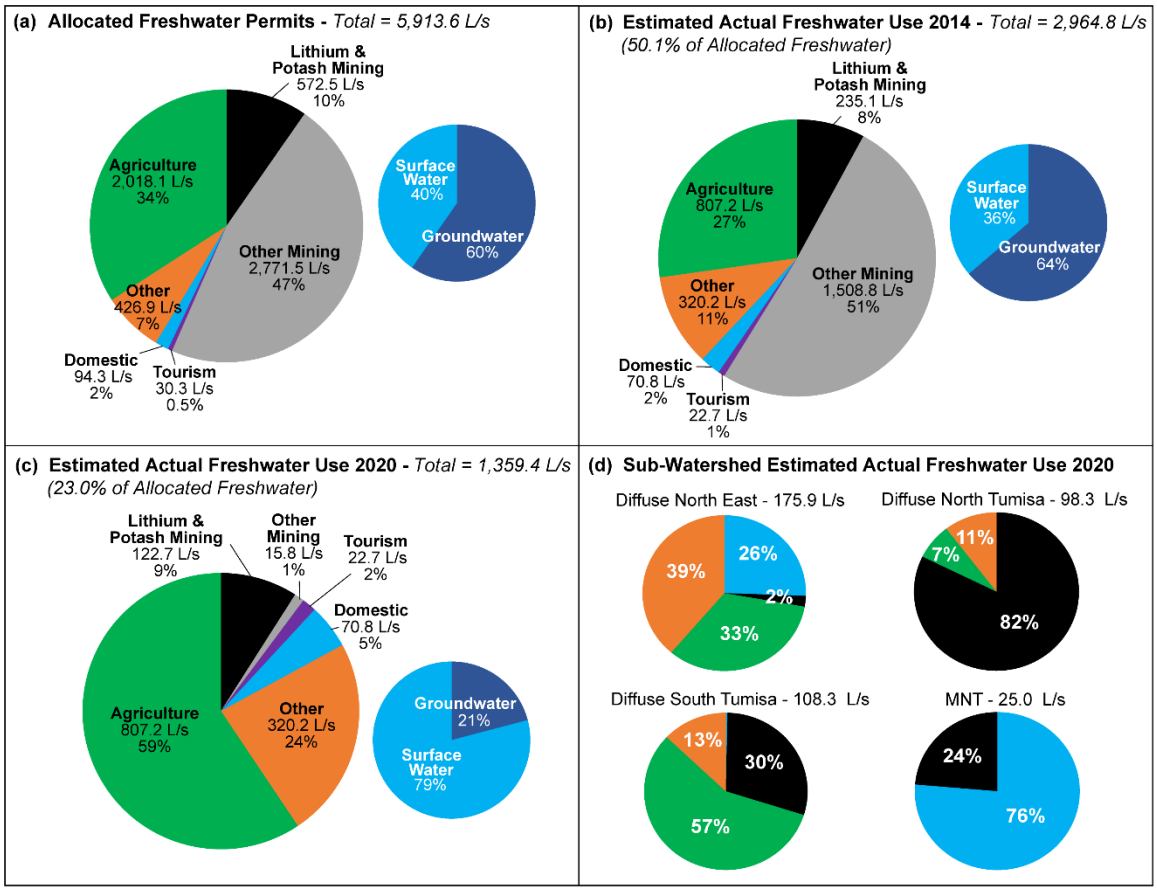

Figure S2. Pie charts of allocated freshwater permits (a); estimated actual freshwater use from 2014 (b); and estimated actual freshwater use from 2020 (c). With additional pie charts representing the percent of surface water (light blue) and groundwater (dark blue). Pie charts in (d) show estimated actual freshwater use from 2020 (L/s) within each sub-watershed zone divided by water use type: lithium mining (black), other mining (grey), agriculture (green), domestic (blue), tourism (purple), and other (orange). Percentages under 1% are not included.

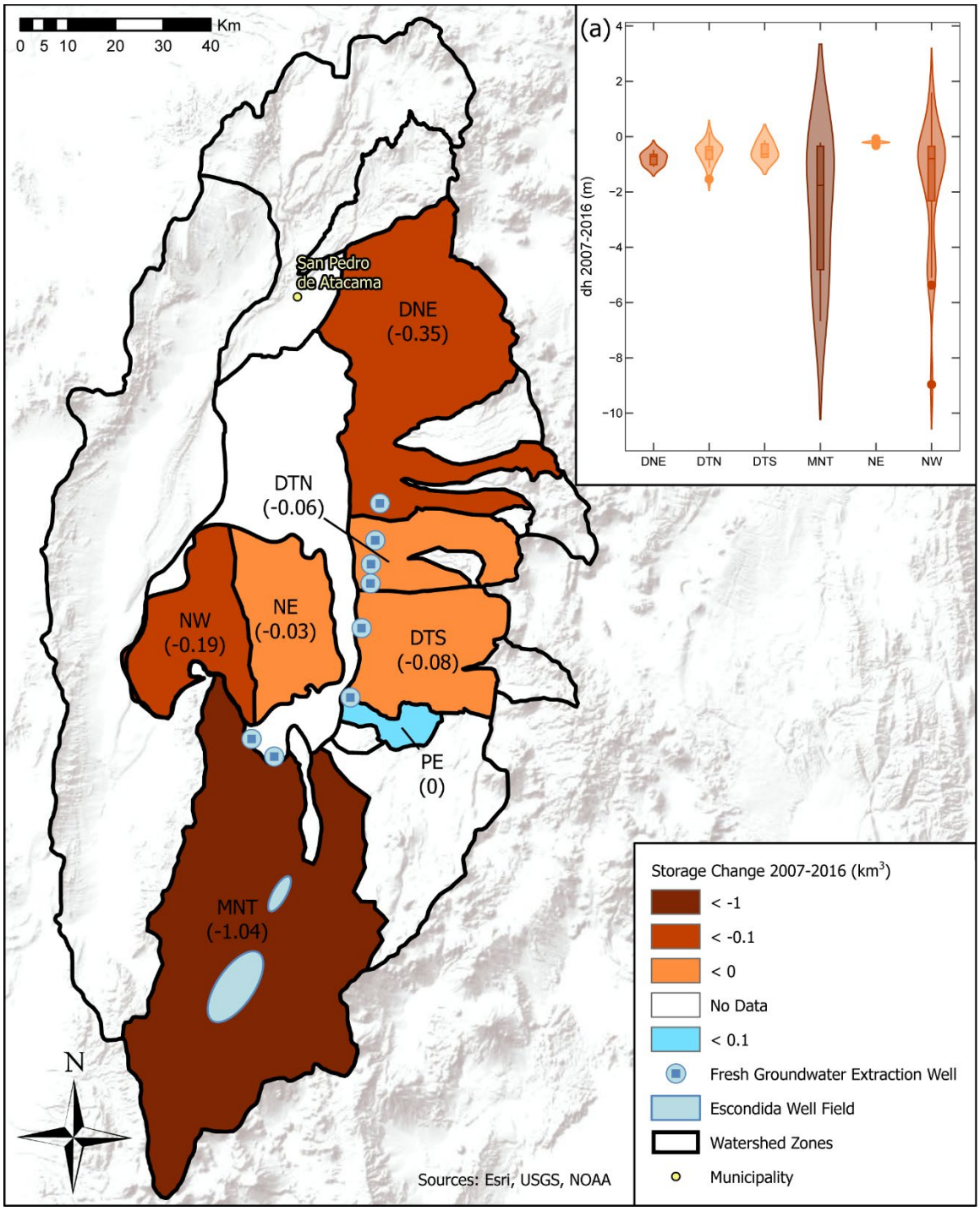

Figure S3. Estimated change in groundwater storage for watershed zones Diffuse North East gw (DNE), Diffuse North Tumisa gw (DTN), Diffuse South Tumisa gw (DTS), Peine (PE), and MNT, as well as nucleus zones East Nucleus (NE) and West Nucleus (NW) in the SdA basin. (a) Violin plot showing the distribution of mean change in the hydraulic head (dh) for monitoring wells located in each watershed or nucleus zone. The method used to obtain these results is provided in **Text S3**.

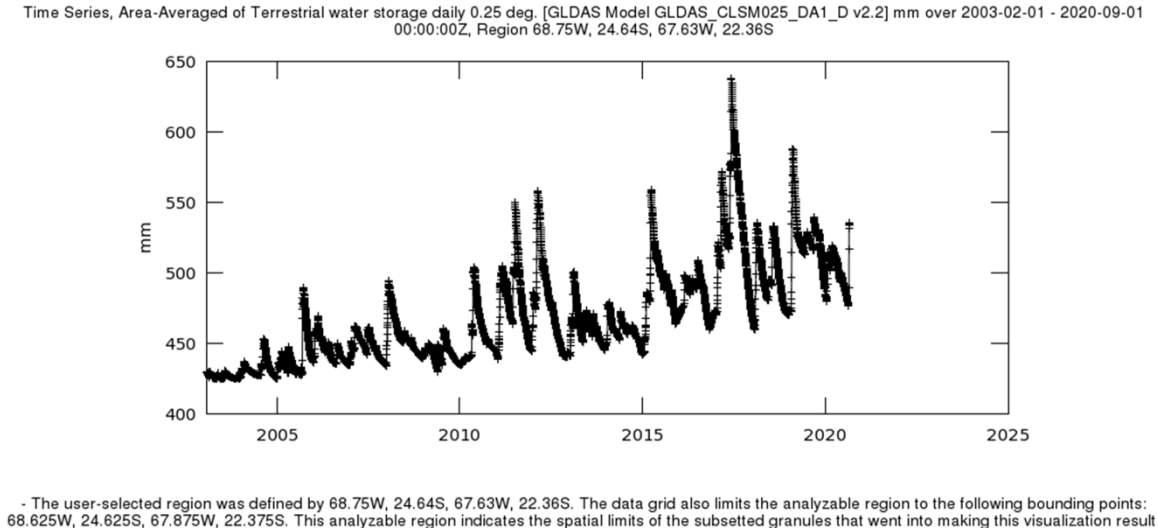

Figure S4. GLDAS v2.2 Land Surface Model output for daily terrestrial water storage change in the Salar de Atacama basin to compare with analysis by Liu & Agusdinata (2020).

Table S1. Summary of geochemical data and results used in this work.

Table S2. Piston-flow physical transit model calculations and results to compare with ^{3}H tracer-based observations of transit times.